

Article

Optimal Strategy to Exploit the Flexibility of an Electric Vehicle Charging Station

Cesar Diaz-Londono ^{1,2,*}, Luigi Colangelo ³, Fredy Ruiz ^{3,4}, Diego Patino ¹, Carlo Novara ³ and Gianfranco Chicco ²

¹ Departamento de Electrónica, Pontificia Universidad Javeriana, Bogotá 110231, Colombia; patino-d@javeriana.edu.co

² Dipartimento Energia “Galileo Ferraris”, Politecnico di Torino, 10129 Torino, Italy; gianfranco.chicco@polito.it

³ Dipartimento di Elettronica e Telecomunicazioni, Politecnico di Torino, 10129 Torino, Italy; luigi.colangelo@polito.it (L.C.); fredy.ruiz@polimi.it (F.R.); carlo.novara@polito.it (C.N.)

⁴ Dipartimento di Elettronica, Informazione e Bioingegneria, Politecnico di Milano, 20133 Milano, Italy

* Correspondence: cesar.diazlondono@polito.it

Received: 11 September 2019; Accepted: 3 October 2019; Published: 10 October 2019



Abstract: The increasing use of electric vehicles connected to the power grid gives rise to challenges in the vehicle charging coordination, cost management, and provision of potential services to the grid. Scheduling of the power in an electric vehicle charging station is a quite challenging task, considering time-variant prices, customers with different charging time preferences, and the impact on the grid operations. The latter aspect can be addressed by exploiting the vehicle charging flexibility. In this article, a specific definition of flexibility to be used for an electric vehicle charging station is provided. Two optimal charging strategies are then proposed and evaluated, with the purpose of determining which strategy can offer spinning reserve services to the electrical grid, reducing at the same time the operation costs of the charging station. These strategies are based on a novel formulation of an economic model predictive control algorithm, aimed at minimising the charging station operation cost, and on a novel formulation of the flexibility capacity maximisation, while reducing the operation costs. These formulations incorporate the uncertainty in the arrival time and state of charge of the electric vehicles at their arrival. Both strategies lead to a considerable reduction of the costs with respect to a simple minimum time charging strategy, taken as the benchmark. In particular, the strategy that also accounts for flexibility maximisation emerges as a new tool for maintaining the grid balance giving cost savings to the charging stations.

Keywords: electric vehicle; flexible demand; model predictive control; spinning reserve

1. Introduction

1.1. Motivations and Aims

Renewable Energy Sources (RES) are increasing worldwide by an average of 2.8%/year [1], thus leading to a possible imbalance between supply and demand in the electrical grid. The RES uncertainty has a significant impact on the scheduling of conventional generation [2] and storage [3]. The main effects of the uncertainty appear both on power system operation and on the need for procuring sufficient reserve capacity to maintain acceptable levels of reliability and security [4].

In recent years, the participation of the demand in operation scheduling and reserve procurement has also increased, with the definition of demand response programmes that involve manual or automatic variation of the demand to reduce the grid risk [5]. The current deployment of the generation and demand resources to improve the power system operation has been represented in the flexibility

framework [6]. There is a vast amount of literature about flexibility definitions and applications; however, according to [7], there is no uniform definition of flexibility. Various definitions of flexibility have been proposed for the generation side and the demand side. In [8], the operational flexibility in power systems is defined as the deviation between the nominal power plant output profile and the actual power output profile. Interactions between flexibility concepts and the diffusion of RES are discussed in [7]. Various forms of grid-side flexibility are addressed in [9]. The thermal generation flexibility for individual generators and for the whole system is defined in [6]. On the other hand, there are viable options to provide flexibility on the demand side. For Thermostatically Controlled Loads (TCL), the aggregate flexibility of a collection of TCLs is defined in [10]. In [11], TCL flexibility is defined considering a geometric approach. A mathematical definition of flexibility for residential demand aggregation is presented in [12], formulated through two demand flexibility indicators by using the binomial probability model. Other formulations refer to water booster pressure systems [13], heat pumps [14], multi-energy systems [15], energy hubs [16], energy storage [17], and the aggregation of electric vehicles (EVs) [18].

In particular, EVs are among the most important deferrable loads in terms of improving RES integration in the grid [19], smoothing the demand curves [20], providing frequency regulation services [21], incrementing self-consumption [22], reducing emissions and supporting green transport [23]. In the last few years, EVs have been becoming a more and more sustainable alternative for private and public road transport [24]. In addition, national governments offer benefits to the customers, in terms of subsidies, financing, or facilities constructions [25].

Typically, an aggregator coordinates EV battery charging. The charging of EV batteries can be managed either in a context where the EVs are not allowed to inject power in the grid, or in the Vehicle-to-grid (V2G) context, where the EVs can inject power into the grid to support grid operation needs [26]. In both cases, appropriate coordination strategies for EV battery charging have to be defined to avoid an inappropriate EV dispatch giving unfavourable impacts to the power networks [27], e.g., with overcurrents in network branches or voltages out of the normal range at network nodes [28].

Moreover, given the huge potential for EV integration, it becomes necessary to assess not only the strategy to streamline the EV battery charging process, but also the possibilities for the electrical grid to take advantage of the charging process. The aim of this paper is to address appropriate dispatching strategies for EV charging, in order to provide additional flexibility to the electrical grid operator. V2G operation is not considered and the related aspects are not discussed.

1.2. Literature Review

A review of EV fleets' aggregation strategies is presented in [29], assessing the potential approaches to provide services to electrical grid operators. The challenge is to define how to manage the EV charging profiles with the purpose of fulfilling the users' requirements and offering a flexibility capacity to the system operator for maintaining the energy balance in the grid.

Specifically, the EV flexibility to reduce the RES power fluctuations is quantified in [30]. The flexibility characterisation of EV charging sessions is addressed in [31], with the introduction of two measures based on flexibility utilisation in terms of energy and duration. A discussion on how the EV batteries management can unlock the potential of using distributed energy resources (DER) is presented in [32]. A definition of EV flexibility is proposed in [33] by adapting the framework introduced in [12] for the flexibility of aggregated residential demand to the case of EVs. EV flexibility is described in [21] in terms of *laxity*, that is, the amount of time left until an EV must charge at its maximum charge rate to reach its minimum scheduled state of charge at the departure time. In [34], the EV recharging flexibility is included in the EV utilisation model together with the type of trip and the possible use of a secondary fuel.

For the EV flexibility assessment, the EV dispatch problem has to be evaluated, also by considering different charging preferences for the EV owners [35]. For instance, a distributed control strategy is

proposed in [36] based on the Lagrangian relaxation. In [37], risk-aware day-ahead scheduling and real-time charging dispatch for EVs are studied. The maximisation of the revenues offering secondary regulation and the maximisation of an EV fleet charging station efficiency are simultaneously addressed in [38]. The charging scheduling of a large number of EVs at a charging station is proposed in [39]. A time-variant storage model for aggregated EVs has been proposed in [40].

Other studies consider the minimisation of the operating energy cost, in combination with the dispatching problem. To this aim, in [41], a multi-objective optimisation framework is proposed. Conversely, [42] focuses on a dynamic programming-based optimisation to provide optimal solutions to charge an EV fleet.

The identification of energy-flexibility and deadline-flexibility referring to EV coordinated charging is carried out in [43]. The coordination can include either the EV owner participation to decide adjustable limits for the EV charging demand [44], or the incorporation of vehicle-originated signals [45].

On the other side, the EV problem has some peculiar characteristics, concerning the uncertainty on arrival and departure times [46]. To this aim, [47] formulates it as an intrinsically stochastic optimisation problem, intended to help the aggregator in reducing expensive peak charging costs or to avoid penalties for not fully charging the batteries of its clients. However, such an implementation proved to be computationally demanding, and characterised by a dimensionality only attackable by using heuristic methods. In [46], a Model Predictive Control (MPC) based power dispatch approach, based on the combination of updated current EV charging information with a short-term forecasting model, addresses the operational cost minimisation while accommodating the EV charging uncertainty. In addition, a framework to address a wide range of uncertainties and variability (e.g., renewable energy, and customer preference) is provided. However, in [48], the MPC strategy together with a stochastic and robust approach is developed for optimising the economic performance of a microgrid with EV integration considering uncertainty in the EV charging request. Interestingly, [49] highlights how, especially concerning uncertain parameters as electricity prices, energy demand and driving patterns, forecasts should always find a balance between long prediction horizons (implying a higher computation time) and how much money can be saved.

1.3. Contributions

This paper proposes a framework for the evaluation and maximisation of power consumption flexibility in Electric Vehicles Charging Stations (EVCS), together with a dispatch strategy that minimises operation costs. An EVCS and its chargers are modelled and controlled as flexible loads. The EVCS is entrusted with charging all the incoming EVs, whose State of Charge (SoC) must reach at least the minimum amount desired by the EV owners at the departure time. From this perspective, the authors follow up the formulation they recently introduced in [50,51] for the operation cost minimisation, and propose a novel charging strategy based on the maximisation of the flexibility provided by EV chargers, taking into account the preferences of the EV users and the uncertainty in the arrival time and SoC. These strategies are compared with a typical minimum time strategy as a benchmark, in order to adjust the profiles of the charging power delivered to the EVs through the battery chargers. Meanwhile, a specific definition of flexibility for EV battery chargers is provided by adapting the concept of operational flexibility in power systems used in [8]. This flexibility definition, differently from [8], leverages the ramp rate in kW/min to describe the variations. Furthermore, considering an analysis with time steps in the order of minutes, for the EV battery chargers, it is possible to adjust the power from the maximum power to zero (and vice versa) in one time step. Subsequently, EV chargers do not require a ramp rate constraint for varying the injected power.

The EV battery charging strategies are based on different optimisation criteria for the charging power profiles, namely:

- minimise the EVCS operation cost, by varying the charging power depending on the energy prices and the charging duration;

- maximise the flexibility capacity (based on Definition 1, presented in Section 2.3), while minimising the EVCS operation cost.

The performance of such an approach depends on the accuracy of the input parameters shaping the devised model. To this aim, the two proposed solutions leverage an MPC that explicitly considers some relevant sources of uncertainty affecting the problem, in order to improve the control performance [52]. However, the performance of such an approach depends on the modeling accuracy of the variables that have an inherent uncertainty [53]. Specifically, in the presented modeling, we consider as the main uncertain parameters the EV arrival time as well as the state of charge at the arrival. In order to provide a practical framework for the definition of the MPC algorithm, the departure time is assumed to be known (from the EV owner request) and is included as a deterministic variable.

In summary, the main contributions of this paper are:

1. a dynamic model of an EV battery charger as a flexible load;
2. a specific flexibility definition for EV battery chargers;
3. a novel formulation for minimising the EVCS operation cost; and
4. a novel optimal strategy that maximises the flexibility capacity of EV battery chargers while minimising the EVCS operation cost that leads to providing spinning reserve services.

1.4. Paper Organisation

The rest of the paper is organised as follows. Section 2 describes the problem faced by an EVCS, how it operates, the charger dynamics model, and introduces the proposed EV flexibility analysis and how to take into account the uncertainties. In Section 3, the EV battery charging strategies are illustrated and thoroughly described. In Section 4, an application case study is shown, along with the related numerical results. Finally, the conclusions are presented in Section 5.

2. The Electric Vehicle Charging Station Problem

An Electric Vehicle Charging Station (EVCS) is composed of various EV battery chargers, to which EVs approach and connect. The problem faced by a typical EVCS for managing the charge of the connected EVs, is twofold:

- (i) chargers scheduling, also taking into account the uncertainty of the EV arrival time and initial state of charge of the EV battery; and,
- (ii) EV load profile management.

The first problem refers to the assignment of a charger to each EV approaching the charging station, as well as their charging time. Secondly, the EV load profile, namely, the charging power delivered by each charger at each time slot defined for the analysis, must also be considered.

In this study, the EVCS works with a centralised infrastructure to collect EV information and to deliver power to each vehicle, i.e., EV battery chargers can be considered as flexible loads in the energy consumption. Consequently, an EVCS can be modeled as an aggregator that is capable of modulating the energy delivered by the chargers. The EV owner willing to recharge the EV battery goes to the charging station and takes part in the program managed by the aggregator. At the departure time specified by the EV owner, the battery will be charged according to the agreement between the aggregator and the EV owner. In the time period in which the EV is managed by the aggregator, the aggregator provides flexibility to the system without the direct action of the EV owner.

In this section, the station operation process and then the EVCS problem formulation are presented. Then, a flexibility evaluation is presented, leading to a novel EV battery charger flexibility definition. For the sake of completeness, Table 1 summarises the notation adopted for the system variables.

Table 1. Notation of the Electric Vehicle Charging Station variables.

Type	Name	Symbol	Units
Independent variable	Time slot	k	-
State variable	State of Charge in charger i	$x_{i,k}$	kWh
Output Variables	Flexibility capacity of the station	F_k	kW
	Flexibility capacity in charger i	$F_{i,k}$	kW
	Power delivered by the station	$P_{T,k}$	kW
	State of Charge in EV $_j$	$SoC_{j,k}$	kWh
Decision Variables	Downward flexibility capacity in charger i	$L_{i,k}^F$	kW
	Power delivered to charger i	$P_{i,k}$	kW
	Upward flexibility capacity in charger i	$U_{i,k}^F$	kW
Parameters	Battery capacity in EV $_j$	C_j	kWh
	Electric vehicle j	EV $_j$	-
	Prediction horizon	H	h
	Number of EV battery chargers	I	-
	Number of EVs	J	-
	Actual SoC in EV $_j$ at a_j	SoC_{j,a_j}	kWh
	Actual SoC in EV $_j$ at d_j	SoC_{j,d_j}	kWh
	Maximum EV $_j$ SoC at the request (at r_j)	\widetilde{SoC}_{j,r_j}	kWh
	Minimum EV $_j$ SoC at the request (at r_j)	\widehat{SoC}_{j,r_j}	kWh
	Minimum desired SoC in EV $_j$ (at d_j)	\widetilde{SoC}_{j,d_j}	kWh
	Maximum possible SoC in EV $_j$ (at d_j)	\widehat{SoC}_{j,d_j}	kWh
	Random arrival SoC in EV $_j$ used in H	\widetilde{SoC}_{j,a_j}	kWh
	EV $_j$ arrival time	a_j	h
	EV $_j$ arrival time in the request	\tilde{a}_j	h
	Energy Price	c_k	\$/kWh
	EV $_j$ departure time	d_j	h
	Time for charging at maximum power	d_m	h
	EV $_j$ charger request time	r_j	h
	Operation time of the station	β	h
	EVs SoC information before a_j	γ	{kWh, ..., kWh}
	Maximum arrival delay	δ	min
	Information provided by the EV $_j$	χ_j	{h, h, kWh, kWh}
	Information provided by all EV	χ_T	set{h, h, kWh, kWh}
	Remuneration Price of the $U_{i,k}^F$	π_k^U	\$/kWh
	Remuneration Price of the $L_{i,k}^F$	π_k^L	\$/kWh
	Schedule of charger i	$\tilde{\zeta}_{i,k}$	{0,1}
	Schedule of all chargers in the station	$\tilde{\zeta}_{T,k}$	set{0,1}
Sampling time	Δt	min	

2.1. Charging Station Operations

The EVCS goal is to charge all the EVs connected to the battery chargers, within their own charging time, achieving a SoC between the minimum SoC desired by the owners at the departure time and full charge (100%). To this aim, an aggregator is responsible for scheduling the charging patterns of an EV group (see Figure 1).

Given a typical EVCS, let us assume that there are I chargers, whose load patterns have been programmed through the aggregator for the next H hours. Notice that these load patterns are affected by uncertainty in the arrival time and the initial SoC of each EV. Furthermore, the operation time of the station is divided into K discrete time intervals with equal length, each of them being a discrete time slot $k = 1, \dots, K$, lasting a sampling time Δt in minutes. Finally, for each day, it is expected to serve J EVs, where for each EV $_j$, its charging time spans from the arrival time a_j to the departure time d_j .

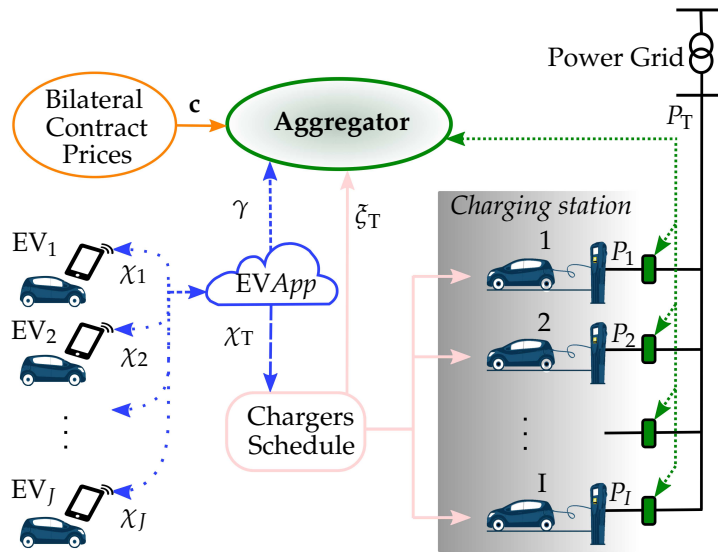


Figure 1. Electric Vehicle Charging Station operation.

A typical EVCS workflow starts with the users, i.e., the EV owners, requesting an available charger, possibly through a mobile application (let us say, *EVApp*), at least one hour before arriving at the station. This recharge request includes the EV_j relevant information, collected in χ_j ,

$$\chi_j = \{\tilde{a}_j, d_j, \widehat{SoC}_{j,r_j}, \widetilde{SoC}_{j,d_j}\}, \quad \forall j = 1, 2, \dots, J; \tag{1}$$

\widetilde{SoC}_{j,d_j} being the minimum SoC desired by the EV_j owner at the departure instant d_j , \widehat{SoC}_{j,r_j} the EV_j SoC at the request time r_j , and \tilde{a}_j the reported arrival time. Then, the EV owner looks for booking an EV charger from \tilde{a}_j to d_j . Finally, all the EV information to be sent to the charger scheduling algorithm is collected in χ_T :

$$\chi_T = \{\chi_1, \chi_2, \dots, \chi_J\}. \tag{2}$$

For the purpose of this study, it is assumed that the actual arrival SoC is higher than zero, i.e., $SoC_{j,a_j} > 0$. In Figure 2, the request time r_j , the expected arrival time \tilde{a}_j , the actual arrival time a_j , and the actual departure time d_j of an EV are presented considering the SoC at the request \widehat{SoC}_{j,r_j} , the expected SoC at the arrival \widetilde{SoC}_{j,a_j} , the actual SoC at the arrival SoC_{j,a_j} , the minimum SoC desired by the owner at the departure \widetilde{SoC}_{j,d_j} , and the actual SoC at the departure SoC_{j,d_j} . Then, notice that the actual arrival SoC and the reported SoC at the request are generally different, i.e., $SoC_{j,a_j} \neq \widehat{SoC}_{j,r_j}$ (see Figure 2a).

Then, the EV arrival SoC and the EV arrival time are uncertain variables that must be managed by the aggregator. Then, the mobile app collects and sends the information $\gamma = \{SoC_{1,r_1}, SoC_{2,r_2}, \dots, SoC_{J,r_J}\}$ to the aggregator. The timings are considered by introducing practical assumption for serving the EV:

- in case of early arrival, nothing changes with respect to the scheduled charging starting instant (\tilde{a}_j); the EV will wait until the scheduled time slot;
- in case of late arrival, up to a given delay δ , the charging procedure can be performed guaranteeing a departure SoC within the requested limits (see feasible condition Equation (16), presented in Section 3.2);
- in case of late arrival, greater than a given delay δ , the vehicle is still accepted, but the requested final SoC cannot be guaranteed; and
- the departure time d_j is fixed by the EV owner request, and is considered as a deterministic variable (see Figure 2b).

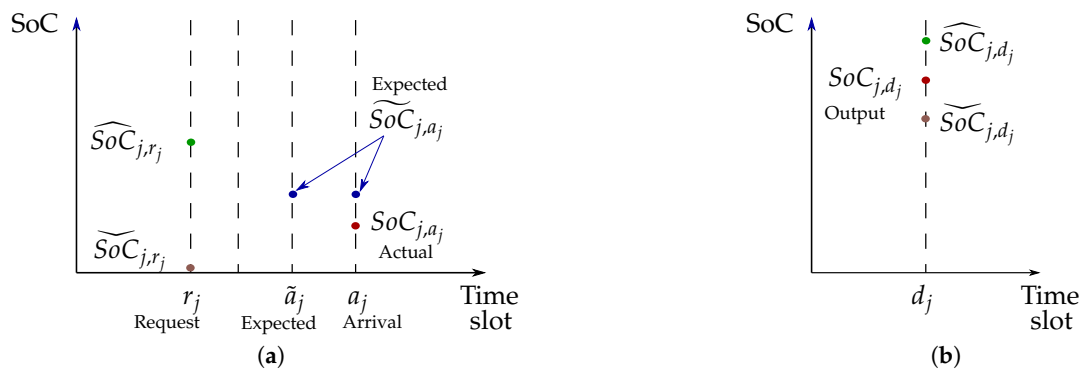


Figure 2. Expected and actual time and state of charge for the j th electric vehicle. (a) Arrival. (b) Departure.

In this context, the arrival time is considered as a random variable uniformly distributed within a given time range around the scheduled time. The arrival SoC is taken into account as a random variable uniformly distributed between zero and the SoC at the request SoC_{j,r_j} .

The aim is to dispatch the J requests to the I chargers, via an allocation algorithm. This algorithm provides two output data sets: (i) the ID_i of the assigned charger (if any), sent to the user, and (ii) a binary state signal $\zeta_{i,k}$, sent to the aggregator. This signal indicates the schedule of the i th charger, i.e., if at the k th time slot, an EV is plugged into it. Hence, at time slot k , it holds:

$$\zeta_{i,k} = \begin{cases} 1, & \text{if the charger } i \text{ has a plugged-in EV,} \\ 0, & \text{if the charger } i \text{ does not have a plugged-in EV.} \end{cases} \quad (3)$$

The decision variables used for the energy dispatch design are the power signals $P_{i,k}$ describing the power delivered by each charger i to the EV connected to it at the time step k . This power can be adjusted for each time slot, in a way consistent with the “Smart charging” concept defined in [54] as charge speed changes in order to match with a control signal or frequency regulation and vehicle parameters. In a smart grid environment, smart charging provides flexibility to the grid, allowing demand response services. Smart charging strategies have been used in [21] by comparing different strategies with the aim of providing frequency regulation services, in [45] in conjunction with the provision of vehicle-originating signals to minimise the variability of the aggregate power pattern with respect to a predefined reference, in [55] to minimise the cost of the charging schedule by taking into account the trading on the intraday electricity market. From a technical point of view, the implementation of dynamic EV charging is discussed in [56] considering different solutions for AC charging, Chademo and Combined Charging System (CCS)/COMBO. Moreover, the Open Charge Alliance has issued the Open Charge Point Protocol [57], in which, while charging is in progress, the connector will continuously adapt the maximum current or power according to the charging profile. Further recent developments on EV charging have been presented in [58].

Therefore, the instant power extracted from the grid, at each time slot k , is:

$$P_{T,k} = \sum_{i=1}^I P_{i,k} \quad \forall k = 1, 2, \dots, K. \quad (4)$$

As a matter of fact, the aim of the aggregator is to define the load profiles $P_{i,k}$ by maximising the operation benefits. To this aim, the EV chargers are considered as flexible loads, in terms of power consumption, which can provide some ancillary services to the electrical grid.

2.2. The Charger Dynamics Model

The SoC dynamics of a vehicle j connected to the charger i , namely, the evolution of the energy stored in the EV battery, can be modeled as:

$$SoC_{j,k+1} = SoC_{j,k} + \Delta t P_{i,k}, \quad (5)$$

where Δt is the sampling time, and $SoC_{j,k}$ is the accumulated energy in the EV battery through the integration of the charging power $P_{i,k}$. No efficiency losses or nonlinearities are considered. Likewise, battery degradation estimation [59] is not considered because the time steps used in the analysis are relatively short (i.e., tens of minutes, for a period of analysis of one day).

Letting $x_{i,k}$ be the state variable representing the SoC of the EV connected to the i th charger, it holds:

$$x_{i,k+1} = \zeta_{i,k} x_{i,k} + \zeta_{i,k} \Delta t P_{i,k}. \quad (6)$$

Hence, when a vehicle is plugged in, namely $\zeta_{i,k} = 1$, the charger dynamics matches Equation (5), i.e., $x_{i,k} = SoC_{j,k}$. Note that, over the course of a day, a charger can charge several EVs. Thus, it is convenient to use the charger SoC as the state variable in the model. As a result, $x_{i,k}$ has a switching behaviour, depending on $\zeta_{i,k}$, and characterised by jumps either from 0 to \widetilde{SoC}_{j,a_j} at each EV arrival, or from SoC_{j,d_j} to 0, at the EV departure. Therefore, the chargers dynamics $x_{i,k+1}$ can have three different conditions:

$$x_{i,k+1} = \begin{cases} x_{i,k} + \Delta t P_{i,k} & \text{if } \bar{a}_j < k < d_j, \\ \widetilde{SoC}_{j,a_j} & \text{if } k = \bar{a}_j, \\ 0 & \text{if } \zeta_{i,k} = 0 \quad \vee \quad k = d_j. \end{cases} \quad (7)$$

The first condition in Equation (7) must hold until the vehicle SoC reaches a value between the minimum SoC desired by the owner and the maximum allowed one. Moreover, considering the third condition in Equation (7), the duration Δt of the time slot k is assumed to be consistent with the time required for an EV finishing the charging process to go away and for another EV to arrive to the same charger.

2.3. Flexibility Evaluation

Considering smart grids, it is possible to provide a service within the energy system by varying the power consumption at the demand side, without affecting significantly the overall service provided by the load. This is known as flexibility [60]. As a matter of fact, a certain degree of flexibility is allowed because there are different ways to charge EV batteries, fulfilling the departure state of charge \widetilde{SoC}_{j,d_j} constraint and maximum power limits.

Generally speaking, flexibility enhances electrical grid security. For example, when a renewable energy source is connected to the grid, fluctuations can imbalance the grid itself. In these cases, a flexible load management system can favorably counteract these effects. Provided that a certain degree of flexibility is available, the system operator can adopt different ancillary services to avoid system instabilities, depending on the component that unbalances the system [10]. In [61], grid ancillary services are classified into four categories based on their response time, as *very short duration*, from milliseconds to 5 min; *short duration*, from 5 min to 1 h; *intermediate duration*, from 1 h to 3 days; and *long duration*, several months. According to [62], the Federal Energy Regulatory Commission definitions of reserves applied in North America are:

- *Regulation*: This service can be provided by units that respond within 15–30 s for fast changes in frequency [63]. In North America, markets like Pennsylvania-New Jersey-Maryland (PJM) [64] and New England [65] call this service Frequency Regulation. Power delivery in this service should last between 10 and 15 min [66].

- *Spinning*: It is provided by units synchronised to the grid. Units must be fully online within 10 min to provide this service. In addition, this service should be maintained for at least 105 min [67].
- *Non-spinning*: It is similar to a spinning reserve; the difference is that a non-spinning reserve does not require the permanent synchronisation of the unit to the grid. Units must be totally available within 10 min. Moreover, spinning reserve is more valuable economically for the system operator because it is usually worth 2 to 8 times as much as a non-spinning reserve on an annual average basis [67]. In addition, this service should be maintained for at least 105 min [66].
- *Replacement*: This service must be supplied within 30 min at the latest, and should be maintained for four hours [68].

From this perspective, the current EV battery charger technology allows for adjusting the power supply within a second; then, EV battery chargers could provide both frequency regulation and reserve services to the grid. However, given that a centralised infrastructure is considered, the communication between the system operator and the EVCS is limited by a few-minute response [69,70]. This implies that, among the many ancillary services, an EVCS can provide spinning or non-spinning reserve, and replacement reserve. In turn, we will focus on spinning reserve, being the most economically valuable one [67]. With the spinning reserve service, a charging station restores the generation and load balance, in the event of a contingency, in a matter of minutes [62]. Then, in order to provide spinning reserve services through an aggregator that takes advantage of the EV flexibility, the concept of flexibility must be evaluated.

Availability of a specific definition of the flexibility of EV battery chargers may help improving the EV schedule and the ancillary services an EVCS can offer. Therefore, a novel definition of flexibility for EV battery chargers is provided as follows.

Definition 1. Given a nominal charging profile $P_{i,k}$ for $k = 1, \dots, K$, the flexibility F_k of an EVCS, for each time slot k , is defined as:

$$F_k = \sum_{i=1}^I F_{i,k} = \sum_{i=1}^I (U_{i,k}^F + L_{i,k}^F), \quad \forall k=1,2,\dots,K, \quad (8)$$

where

$$U_{i,k}^F = \begin{cases} P_{i,\max} - P_{i,k} & \text{if } \zeta_{i,k} = 1 \wedge k < d_m, \\ 0 & \text{if } x_{i,k} = x_{i,\max} \vee x_{i,k} = 0 \vee k \geq d_m, \end{cases} \quad (9a)$$

$$L_{i,k}^F = \begin{cases} P_{i,k} & \text{if } \zeta_{i,k} = 1 \wedge k < d_m, \\ 0 & \text{if } x_{i,k} = x_{i,\max} \vee x_{i,k} = 0 \vee k \geq d_m. \end{cases} \quad (9b)$$

Note that the flexibility is the maximum power deviation that the profile can reach either upward or downward.

Therefore, a charger is said to be upward-flexible ($U_{i,k}^F > 0$), when it can increase the power injected to the connected EV. It happens whenever the power delivered by the charger is lower than $P_{i,\max}$, and the $SoC_{j,k} < x_{i,\max}$. On the other hand, a charger is downward-flexible ($L_{i,k}^F > 0$) if it can decrease the power injected to the connected EV (see Equation (9b)). Since the V2G concept is not considered, the charging station problem works only in a unidirectional system, thus $P_{i,k} \geq 0$.

A detailed view of EV battery charger flexibility is presented in Figure 3. The structure of the figure is consistent with the framework presented in [32] for EVs, which considers SoC on the vertical axis, while the operational flexibility framework introduced in [8] (not referring to EVs) has a similar representation, but the vertical axis is expressed in MW for power system studies. In particular, Figure 3a shows the EV SoC behaviour during the charging time. The continuous green line is an example of an EV Generic Charging (GC) profile, and the dashed-blue and the dash-dotted red lines represent the limits of the SoC area. These limits are described by two charging profiles. First, of all,

the Minimum Time (MT) strategy (dashed blue line), obtained by injecting the maximum power $P_{i,max}$, immediately at the EV arrival time, until the full charge.

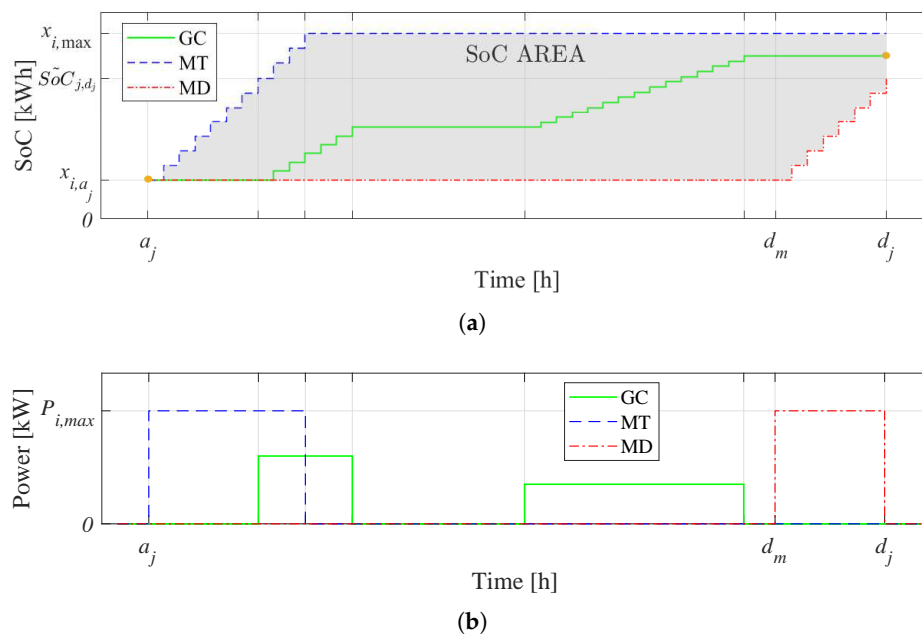


Figure 3. SoC area in an EV charger. (a) SoC area with an example of a SoC profile (continuous green line). (b) Charging power profile.

Secondly, the Most Delayed (MD) strategy (dash-dot red line) suggests that, starting from time d_m , only the maximum allowed power $P_{i,max}$ lets the SoC reach the (minimum) desired departure value \widetilde{SoC}_{j,d_j} (in this case, no flexibility is possible from d_m to d_j). Figure 3b depicts the power injected by strategies GC, MT, and MD for creating the SoC area. Note that there are no idle losses due to the short time horizon, and no negative power flows are considered as this work does not take into account V2G applications.

In short, the upward flexibility is the capacity of increasing the charging power up to $P_{i,max}$, while the downward flexibility is the capacity of charging with lower power or renounce to charge. Finally, the EV should depart with a charge level $x_{i,d_j} \in [\widetilde{SoC}_{j,d_j}, x_{i,max}]$, where $x_{i,max}$ corresponds to the full charge condition.

In addition, in Figure 4, the flexibility areas for the three strategies are shown, highlighting the upward (U) and the downward (L) flexibility. Although the downward (L) flexibility is positive, for better representation, it is plotted as a negative value to indicate a power reduction, i.e., $-L$ is depicted. In the MT case (Figure 4a), it is possible to achieve downward flexibility ($-L_{MT}$) only, due to the possibility of reducing power (up to $P_{i,max}$). However, after fully charging the EV, no flexibility is allowed. In the MD case (Figure 4b), it is possible to achieve upward flexibility (U_{MD}) only, due to the possibility of increasing power to $P_{i,max}$. However, after d_m , charging at maximum power $P_{i,max}$ is needed to reach \widetilde{SoC}_{j,d_j} . Consequently, no charging flexibility is allowed after that instant. In the GC case (Figure 4c), the upward (U_{GC}) and the downward ($-L_{GC}$) flexibilities are shown. The filled parts indicate the area where the power charging profiles can be adjusted, following profiles of $P_{i,k} \in [0, P_{i,max}]$ that guarantee not to violate the constraints. It is noteworthy that the SoC might also remain constant for a certain period, e.g., when the EV is not charged, according to the aggregator needs.

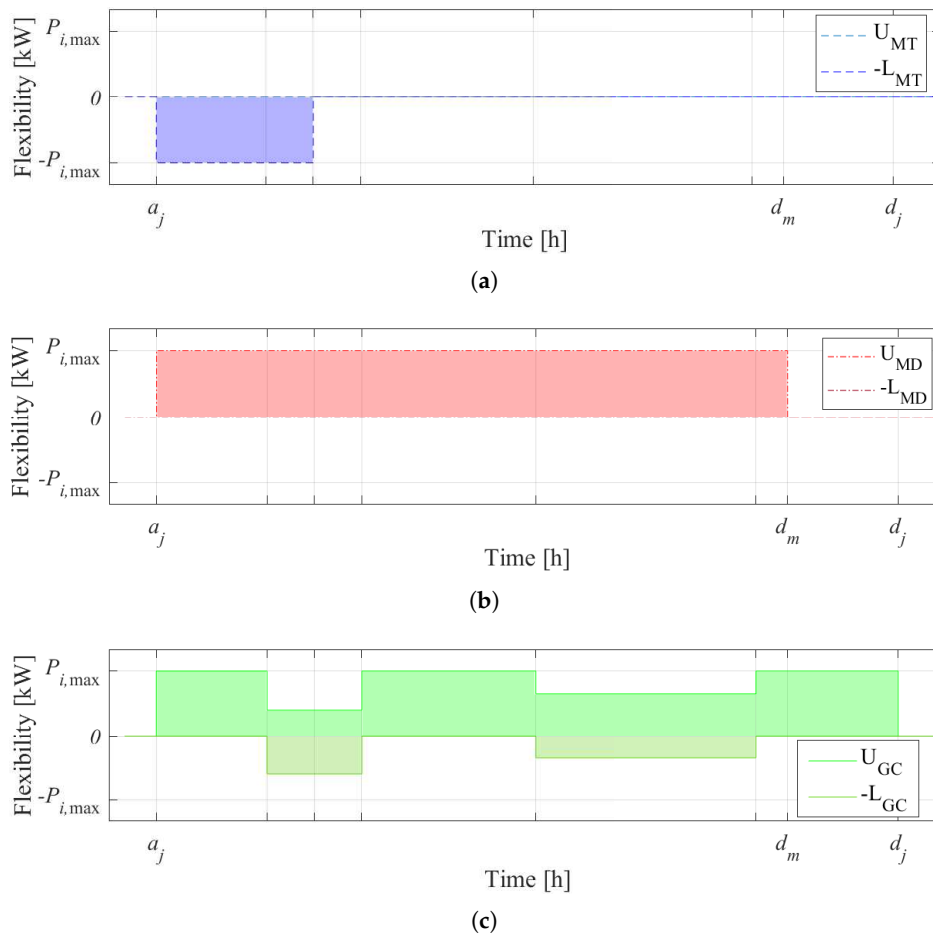


Figure 4. Flexibility in an EV charger. (a) Flexibility area for MT. (b) Flexibility area for MD. (c) Flexibility area for GC.

As a result, the flexibility assessment turns out to be crucial to maintaining the electrical grid balance. Consequently, the aggregator can provide a balancing service, restricted by the defined GC profiles, admitting the possibility of having zero flexibility capacity in some time slots. Note that, with the defined GC power exemplified in Figure 3b, it is possible to achieve a flexibility $F_{i,k} = P_{i,k}$ at all plugged-in time, i.e., all time steps (see Figure 4c).

Therefore, the charging station problem, given the power design variables (namely, the power supply sequence $P_{i,k}$ and the flexibility capacities $U_{i,k}^F$ and $L_{i,k}^F$), consists of selecting the optimal power load profile $P_{i,k}^*$ for each charger i , for all the time slots up to the total operation time of the charging station β . Interestingly, the aggregation decision might also be based on the electricity price c_k and reserve prices, assumed to be known from bilateral contracts (with the aggregator that manages the charging station) and variable hourly. As such, no uncertainty is considered for these prices. In this framework, the optimisation problem formulation will aim at guaranteeing a flexibility capacity, while minimising operational costs, and ensuring a departure SoC within the requested limits for each EV.

3. Solution Strategies

In this section, three strategies to attack the EV charging station problem are discussed:

1. Minimum Time (MT), as a standard approach, here adopted as a benchmark;
2. economic Model Predictive Control (eMPC), whose basics were presented in our previous works [50,51]; and,
3. Optimal Control with minimum Cost and maximum Flexibility (OCCF), a novel strategy based on the Definition 1 presented in Section 2.3.

In the eMPC and OCCF strategies, uncertain parameters such as EVs' initial SoC at the arrival and their arrival times are considered. Both strategies are based on MPC formulations. The MPC strategy (also known as Receding Horizon Control) makes explicit use of a plant model to obtain the optimal control signal by minimising an objective function. MPC exploits forecast values together with new information to establish the future evolution of the system, handling the constraints in an efficient way. The main advantages of the MPC strategy are: (i) it introduces feed-forward control implicitly, to compensate disturbances and measurement noise rejection; (ii) it is not conceptually complex to treat the constraints over inputs, states, outputs and slew-rate variables; (iii) single-variable and multi-variable cases are easily treated; and (iv) it is appropriate to address single-objective and multi-objective control, and signal following.

3.1. Minimum Time as a Benchmark

A straightforward strategy to charge EVs in an EVCS is based on the charging time minimisation. In short, each vehicle is charged at the maximum allowed power $P_{i,\max}$, until it reaches its full capacity $SoC_{i,\max}$. However, this strategy does not take into account the time-varying energy price, nor the possibility to provide ancillary services to the electrical grid. To sum up, the charging power $P_{i,k}$ is determined as:

$$P_{i,k} = \begin{cases} P_{i,\max} & \text{if } 0 < x_{i,k} < x_{i,\max}, \\ 0 & \text{otherwise,} \end{cases} \quad (10)$$

where $x_{i,\max}$ is the maximum admissible SoC in the EV_{*j*}. For example, by considering an EVCS with charging power levels 2 (semifast) and 3 (fast), and an EV with a battery capacity of 50 kWh, the charging time is expected to be around six hours for level 2 and one hour for level 3 [71], depending on the SoC at the arrival. Note that, for achieving the minimum SoC \widetilde{SoC}_{j,d_j} (full SoC capacity with this strategy) at the departure time, only the EV_{*j*} charging feasibility in a time-span from a_j to d_j is required. This is clarified below.

3.2. Economic Model Predictive Control

A novel formulation for the cost minimisation strategy based on a MPC algorithm is presented in this section. The MPC path to the solution of the charging station problem looks for adjustments in the injected power $P_{i,k}$, at every time slot k , in each charger i , considering the time-variant energy prices c_k , the uncertainty in the EV arrival time and SoC at the arrival time, i.e., a_j and SoC_{j,a_j} . Hence, the optimality here refers to a charging profile that minimises the EVCS operation costs, while guaranteeing for all EV_{*j*} the minimum \widetilde{SoC}_{j,d_j} at the departure time d_j . Thus, by recalling Equation (3), Equation (4) and Equation (7), it holds:

$$\min_{P_{i,k}} \quad \Delta t \sum_{k=0}^{H-1} \left(c_k \sum_{i=1}^I P_{i,k} \right) \quad (11a)$$

$$\text{s.t.} \quad x_{i,k+1} = \begin{cases} x_{i,k} + \Delta t P_{i,k} & \text{if } \tilde{a}_j < k < d_j, \\ \widetilde{SoC}_{j,a_j} & \text{if } k = \tilde{a}_j, \\ 0 & \text{if } \zeta_{i,k} = 0 \quad \forall \quad k = d_j, \end{cases} \quad (11b)$$

$$\widetilde{SoC}_{j,d_j} \leq x_{i,d_j} \leq \widehat{SoC}_{j,d_j},$$

$$0 \leq P_{i,k} \leq P_{i,\max},$$

$$0 \leq x_{i,k} \leq x_{i,\max},$$

$$\forall k = 1, 2, \dots, H, \quad i = 1, 2, \dots, I, \quad j = 1, 2, \dots, J.$$

Notice that the dynamic constraint considers the reported arrival time \tilde{a}_j in the request, and a random initial state \widetilde{SoC}_{j,a_j} given with a uniform distribution between the minimum \widetilde{SoC}_{j,r_j} and the SoC at the request time \widetilde{SoC}_{j,r_j} . Therefore, the actual arrival SoC is lower than the one at the request,

i.e., $SoC_{j,a_j} < \widehat{SoC}_{j,r_j}$. In addition, the actual arrival time a_j is known within the time interval previous to the connection of the EV to the charger.

In Equation (11), the aggregator problem is an optimal control strategy in open loop. Specifically, for the k th time slot, $x_{i,k}$ is the state variable corresponding to the i th charger SoC, while $P_{i,k}$ is the commanded variable corresponding to the delivered power profile. It is worthwhile to notice that the problem parameters in Equation (11) are affected by uncertainties on arrival time and SoC of the EVs. An open loop strategy cannot consider the future unknown behaviors, leading to possible unfeasibilities in the optimal solution. Therefore, the solution strategy should take these uncertain behaviors into account, and possibly recompute the control signal, even at each time step if needed. For this reason, a model predictive control strategy is proposed, following the receding horizon principle. In a nutshell, the idea is to compute, at time k , an optimal control sequence, over the complete time-interval, e.g., $[k, k + H - 1]$, taking into account the current and future constraints. Nevertheless, only the first step in the resulting optimal control sequence is applied. Then, in the next time slot $k + 1$, once the chargers' information is updated with the new measures, the aggregator recomputes the sequences, thus iterating the process.

Thereupon, in the eMPC problem framework, finding the problem solution requires to analyse, at each time slot, the system dynamics, and the future energy prices, while taking into account the current SoC and the arrival and departure times for each vehicle, as per Equation (11). Notice that both uncertain parameters (the arrival time and the initial SoC) are revealed when the EV arrives at EVCS and is plugged in. After this, there is no more uncertainty in the EV state, leading to an appropriate power profile schedule. As indicated in Section 1.3, using time slots of the order of minutes, the possible variations with respect to the scheduled values are compensated in the first time slot of the MPC algorithm.

The parameters (price sequence c_k , reported arrival time \tilde{a}_j , and SoC at the request \widehat{SoC}_{j,r_j}) are assumed to be known, while $P_{i,max}$ depends on the maximum power that either the charger can deliver, or the EV can accept. Moreover, the actual SoC_{a_j} is known when the EV connects to the charger; then, the prediction model is developed considering the expected value \tilde{a}_j for each EV (see Figure 2a). Regarding $\zeta_{i,k}$, it is determined by using the requested times \tilde{a}_j and d_j . Notice that both the arrival time and arrival SoC of each EV can be different at the actual connection time step.

The eMPC strategy looks for input sequences minimising the total cost of the EVCS, as per Equation (11), in a time window of H hours, for each EV. To this aim, the dynamic constraint Equation (11b), i.e., when $\zeta_{i,k} = 1$ while $\tilde{a}_j < k < d_j$, can be expressed in an extended form as:

$$\hat{x}_{k+1} = \underbrace{\text{diag}(\zeta_{i,k})}_{A_k} \hat{x}_k + \underbrace{\text{diag}(\zeta_{i,k} \Delta t)}_{B_k} \hat{P}_k, \quad (12)$$

where

$$\hat{x}_k = [x_{1,k} \ x_{2,k} \ \dots \ x_{I,k}]^T, \quad \hat{P}_k = [P_{1,k} \ P_{2,k} \ \dots \ P_{I,k}]^T. \quad (13)$$

Hence, the evolution of all x_i , throughout the prediction horizon H , reads:

$$\mathbf{x} = \mathbb{A} \hat{x}_k + \mathbb{G} \mathbb{P}, \quad (14)$$

where

$$\mathbf{x} = \begin{bmatrix} \hat{x}_{k+1} \\ \hat{x}_{k+2} \\ \vdots \\ \hat{x}_{k+H} \end{bmatrix}, \quad \mathbb{P} = \begin{bmatrix} \hat{P}_k \\ \hat{P}_{k+1} \\ \vdots \\ \hat{P}_{k+H-1} \end{bmatrix}, \quad \mathbb{A} = \begin{bmatrix} A_k \\ A_k A_{k+1} \\ \vdots \\ A_k \cdots A_{k+H-1} \end{bmatrix}, \quad (15)$$

$$\mathbb{G} = \begin{bmatrix} B_k & 0 & 0 & 0 \\ A_{k+1} B_k & B_{k+1} & 0 & 0 \\ \vdots & \vdots & \ddots & 0 \\ A_{k+1} \cdots A_{k+H-1} B_k & A_{k+2} \cdots A_{k+H-1} B_{k+1} & \cdots & B_{k+H-1} \end{bmatrix}.$$

Notably, the system in Equation (14) is time variant, since $x_{i,k+1}$ in the prediction horizon has a switching behavior. In addition, \hat{x}_k is the initial condition, it contains the current EV SoC when $\xi_{i,k}=1$ and zero when $\xi_{i,k}=0$. Moreover, the cost function in Equation (11a) is linear in $P_{i,k}$, and the dynamic Equation (14) is a linear equality constraint in $P_{i,k}$. Furthermore, the other constraints in Equation (11) are linear inequalities that bind the feasible region described as a polytope. Then, the aggregator deals with a Linear Programming (LP) convex problem, which can be efficiently solved by Simplex or interior point methods.

Furthermore, it is noteworthy that the devised eMPC strategy might be affected by feasibility issues related to the charging time. As a matter of fact, it is assumed that the resulting charging time, when the eMPC formulation is employed, must be greater or equal than in the Minimum Time charging case. Thereby, the optimal control problem Equation (11) is said to be feasible if and only if:

$$(d_j - a_j)P_{i,\max} > \widetilde{SoC}_{j,d_j} - SoC_{j,a_j}. \quad (16)$$

In short, Equation (16) implies that the time an EV spends plugged-in (from a_j to d_j) is at least enough to charge it with maximum power $P_{i,\max}$. From the feasibility condition Equation (16), how the economic MPC strategy will generally increase the time spent at the charging station premises appears, although a certain reduction of the recharge operating costs is guaranteed. Regarding the uncertain parameters, they must be inside the feasible region; otherwise, the problem is not feasible and the EV cannot be charged up to the minimum state \widetilde{SoC}_{j,d_j} . However, an EV that arrives too late with respect to the request is still allowed to be charged, without guaranteeing that the minimum \widetilde{SoC}_{j,d_j} will be reached.

In order to assess the complexity of the problem, it can be noticed that:

- the size of the decision and the state variables, $P_{i,k}$ and $x_{i,k}$ respectively, is $I \cdot H$;
- the number of constraints in $P_{i,k}$ is $2 \cdot I \cdot H$, for each time slot, half for the lower bounds, and half for the upper bounds;
- the number of constraints in $x_{i,k}$ is $3 \cdot I \cdot H$, for each time slot; equally allocated among the lower and the upper bounds, and the charger dynamics;
- the number of constraints in x_{i,d_j} , related to the minimum SoC requirement \widetilde{SoC}_{j,d_j} at the departure, is I .

It is evident that the problem complexity grows linearly with H . This implies that, by scaling up the number of chargers, the number of constraints and decision variables would also increase accordingly, possibly impinging on the optimisation solution efficiency.

3.3. Optimal Control with Minimum Cost and Maximum Flexibility

In this subsection, a novel strategy for the charging station problem solution, based on flexibility maximisation, is proposed. The aim of this novel strategy is to offer a power flexibility capacity to the electrical grid, while guaranteeing the minimum SoC requirement \widetilde{SoC}_{j,d_j} at the departure time. The uncertainty in the EV arrival time and SoC at the arrival time are considered as in Section 3.2.

According to Definition 1, the concept of (upward or downward) flexibility F_k is determined with respect to a nominal charging profile $P_{i,k}$, whereas $F_k = 0$ implies that no ancillary service may be offered to the grid. Hence, it could be crucial to set-up a charging strategy that always guarantees a certain amount of flexibility capacity. To pursue such an objective, two parallel paths can be developed, involving the flexibility as either an optimisation constraints or part of the cost function.

In fact, on the one hand, the optimisation constraints in Equation (11b) can be properly rephrased, in order to impose a minimum flexibility capacity to the chargers. Specifically, such an approach envisages two possible strategies for the constraint reformulation. In the first strategy, the equation in Equation (11b) binding the vehicle charging power $P_{i,k}$ is adapted to guarantee a certain degree of flexibility $F_{i,k}$,

$$F_{i,k} \leq P_{i,k} \leq P_{i,max} - F_{i,k}, \quad \text{where} \quad F_{i,k} = \frac{F_k}{\sum_{i=1}^I \zeta_{i,k}}, \quad (17)$$

$F_{i,k}$ being a parameter defining the flexibility requested to charger i at time slot k , while F_k is the overall flexibility offered by the EVCS, at the k time slot. It is worth noting that the constraint Equation (17) implies the same upward and downward flexibility, achievable for $\sum_{i=1}^I \zeta_{i,k} \geq 1$. Moreover, all the I chargers provide the same flexibility level at each time slot.

The second strategy for the constraints reformulation mainly consists of adding a new constraint to Equation (11b), binding the aggregated power $P_{T,k}$, yet leaving unmodified the single-vehicle power limits. Such a further constraint reads:

$$F_k \leq P_{T,k} \leq \sum_{i=1}^I (\zeta_{i,k} \cdot P_{i,max}) - F_k, \quad \forall k=1,2,\dots,K. \quad (18)$$

Note that, by introducing Equation (18), the flexibility of each charger can be different. Indeed, the idea is to impose a gap in the power requested to the grid.

Finally, in spite of its capability to grant some level of flexibility, and, in turn, some extra energy service to the grid, a solution of the EVCS optimisation problem including the constraints Equation (17) or Equation (18) might result in being infeasible. In fact, the maximum flexibility $F_{C_{T,k}}$ achievable by the EVCS is not known in advance. Indeed, this capacity depends on the state behavior.

On the other hand, in a second path to approach the charging problem improving the flexibility capacity, the optimisation problem formulation is re-framed according to an optimal control strategy, aimed to simultaneously maximise the charging flexibility and minimise the operational cost of the EVCS. This formulation assumes that remuneration factors π_k^U (upward) and π_k^L (downward) for the flexibility offered by the station are driven by prices.

To sum up, the aggregator deals with an optimal control problem, i.e.:

$$\min_{P_{i,k}, U_{i,k}^F, L_{i,k}^F} \Delta t \sum_{k=0}^{H-1} \left(c_k \sum_{i=1}^I P_{i,k} - \pi_k^U \sum_{i=1}^I U_{i,k}^F - \pi_k^L \sum_{i=1}^I L_{i,k}^F \right) \quad (19a)$$

$$\text{s.t.} \quad x_{i,k+1} = \begin{cases} x_{i,k} + \Delta t P_{i,k} & \text{if } \tilde{a}_j < k < d_j, \\ \widetilde{SoC}_{j,d_j} & \text{if } k = \tilde{a}_j, \\ 0 & \text{if } \zeta_{i,k} = 0 \quad \vee \quad k = d_j, \end{cases} \quad (19b)$$

$$\widetilde{SoC}_{j,d_j} \leq x_{i,d_j} \leq \widehat{SoC}_{j,d_j}, \quad (19c)$$

$$L_{i,k}^F \leq P_{i,k} \leq \zeta_{i,k} (P_{i,max} - U_{i,k}^F), \quad (19d)$$

$$0 \leq U_{i,k}^F \leq P_{i,max}, \quad (19e)$$

$$0 \leq L_{i,k}^F \leq P_{i,max}, \quad (19f)$$

$$0 \leq x_{i,k} \leq x_{i,max}, \quad (19g)$$

$$\forall k = 1, 2, \dots, H, \quad i = 1, 2, \dots, I \quad j = 1, 2, \dots, J.$$

In this case, the aggregator decision variables are the optimal profile $P_{i,k}$ and the flexibilities $U_{i,k}^F$ and $L_{i,k}^F$ of the i th charger. Concerning $U_{i,k}^F$ and $L_{i,k}^F$, in Equation (19), two new constraints are introduced. Indeed, $U_{i,k}^F$ and $L_{i,k}^F$ are considered as lower-bounded by zero and upper-bounded by $P_{i,\max}$. Then, the charging power $P_{i,k}$ is always positive.

This formulation allows for finding solutions that maximise both upward $U_{i,k}^F$ and downward $L_{i,k}^F$ flexibilities. Furthermore, the resulting charging strategy may lead to non-symmetric flexibility capacities, consistently with Definition 1.

Finally, the dynamic constraint for the SoC in $x_{i,k}$ being in line with Equation (11b), its evolution can be again consistently expressed as per Equation (14). Taking into account the discussion after Equation (15) about linearity in the problem Equation (11), note also that the cost function in Equation (19a) is a linear function of $P_{i,k}$ as Equation (11a) and the new constraints are linear as well. Then, like for the eMPC case, the aggregator faces an LP convex problem. Similarly, the feasibility condition presented in Equation (16) also holds for the problem formulation Equation (19). From this perspective, it can be noticed how the approach Equation (19), in the worst-case scenario, would not allow any flexibility, thus reducing to the same outcome of the eMPC model in Equation (11).

To conclude, it is expected that this innovative OCCF strategy, with flexibility maximisation, generates higher expenses for the EVCS with respect to the eMPC one because the energy value is not the only element of the cost function. Nonetheless, it can provide to the grid a significant flexibility capacity. In turn, such additional flexibility would allow the generation of relevant extra revenues for the EVCS, due to the aggregator service in maintaining the electrical grid balance.

4. Case Study and Results

In this section, a case study with several simulation results is presented, with the aim of evaluating the performance of the three charging strategies:

1. Minimum time (MT).
2. Economic MPC (eMPC).
3. MPC with minimum cost and flexibility maximisation (OCCF).

For this purpose, the EV charging profiles $P_{i,k}$, the charger SoC $x_{i,k}$, the flexibility capacities $L_{T,k}^F$ and $U_{T,k}^F$, and the resulting operation costs for each strategy are compared. An EVCS sampling time of $\Delta t = 10$ min is employed in order to provide spinning reserve service. The solution of the resulting optimization problems is obtained with the CVX package [72]—specifically, the convex LPs in Equation (11) and Equation (19), with a one-day simulation length, thus $\beta = 24$ h (144 time steps).

The EVs considered in the case study are the electric taxis that circulate in Bogotá, Colombia. In fact, all the EVs have the same characteristics, namely, they are BYD e6 cars with a battery capacity of 80 kWh and a nominal charging rate of 8 kW. They can also support a fast charging rate of 50 kW [71]. Concerning the minimum desired SoC at the departure, a full charge condition is requested in all the simulations ($\widetilde{SoC}_{j,d_j} = \widetilde{SoC}_{j,d_j}$), in order to make a meaningful comparison with the MT strategy, in which the EVs are fully charged at the end of the period. Regarding the uncertain parameters, the actual arrival time a_j for each EV is generated as a sample of a random variable with uniform distribution, mean value given by the declared arrival time \tilde{a}_j , and support between $\tilde{a}_j \pm \delta$, with $\delta = 20$ min. This variability leads to a feasible problem, considering that the minimum interval an EV owner can book a charger is 2 h (see Equation (16)). Then, in the worst case, a charging time of 1 h and 40 min is enough time for charging an EV with the given characteristics, by injecting the maximum feasible power. Moreover, the actual EV _{j} arrival state of charge SoC_{j,a_j} is generated as a sample of a uniform distribution with support between the reported SoC at the request \widetilde{SoC}_{j,r_j} and \widetilde{SoC}_{j,r_j} , where, without loss of generality, \widetilde{SoC}_{j,r_j} is a random number between 15% and 40% of the EV capacity, and $\widetilde{SoC}_{j,r_j} > 0$. In addition, for the MPC algorithm, the expected value \widetilde{SoC}_{j,a_j} is considered as a random value lower than \widetilde{SoC}_{j,r_j} and higher than zero.

The adopted simulation parameters, characterising the optimisation models, are reported in Table 2. Concerning the optimisation scenario configuration, a prediction horizon of $H = 6$ h (36 time steps) is assumed as the maximum time an EV can spend at the charging station premises. Furthermore, in these tests, two different energy price sequences are considered. They are hourly sampled time-variable prices, named $c_{1,k}$ (Figure 5a) and $c_{2,k}$ (Figure 11), corresponding to real data taken from the Colombian stock market. They allow for assessing the potential diversity in the aggregator responses. Moreover, in line with the Colombian energy market regulation and without loss of generality, the benefit price granted to the EVCS for its flexibility capacity is assumed to have the same price as the traded energy [73], i.e., $\pi_k^U = \pi_k^L = c_k$.

Table 2. Case study simulation parameters.

Name	Symbol	Value	Notes
EVCS sample time	Δt	10 min	-
Operation time of the station	β	24 h	(144 iterations)
Maximum arrival delay	δ	20 min	-
Prediction horizon	H	6 h	(36 iterations)
Battery capacity in EV _j	C_j	80 kWh	-
Charging power (time slot k)	$P_{i,k}$	8 kW	Semifast (Level 2)
Charging power (time slot k)	$\widetilde{P}_{i,k}$	50 kW	Fast (Level 3)
Minimum SoC in EV _j (at departure)	\widehat{SoC}_{j,d_j}	80 kWh	$x_{i,d_j} = C_j$
Energy price 1 (time slot k)	$c_{1,k}$	0.0577 \$/kWh 0.0252 \$/kWh	Mean value Std dev.
Energy price 2 (time slot k)	$c_{2,k}$	0.0614 \$/kWh 0.0115 \$/kWh	Mean value Std dev.
Remuneration price (time slot k)	π_k^U, π_k^L	$c_{1,k}$ or $c_{2,k}$	-

4.1. Charger Flexibility Analysis

In order to perform a worthwhile analysis of the proposed charging strategies, a simulation campaign is set up, considering first a deterministic scenario and then a setting with uncertainty. The simulated charging station considers three chargers, and 11 EV re-charge requests, with the energy price sequence $c_{1,k}$, as per Table 2. Specifically, Table 3 lists the 11 electric taxis requests, with their request arrival time \tilde{a}_j and departure time d_j , their SoC at the request $\widehat{SoC}_{r,j}$, and the identification number ID_i of the charger assigned by the scheduler. The actual information on the arrival time a_j and arrival state of charge $SoC_{a,j}$ is also reported.

Table 3. EV charger schedule.

EV _j	EV ₁	EV ₂	EV ₃	EV ₄	EV ₅	EV ₆	EV ₇	EV ₈	EV ₉	EV ₁₀	EV ₁₁
$\widehat{SoC}_{r,j}$	28.0	23.0	32.0	13.0	23.0	17.0	22.0	26.0	24.0	18.0	30.0
$SoC_{j,a,j}$	8.4	21.7	17.1	7.6	6.9	3.2	3.4	n/d	6.6	16.3	21.5
\tilde{a}_j	3:30	5:30	5:30	7:30	10:30	10:30	11:30	13:30	15:30	16:30	20:30
a_j	3:40	5:20	5:40	7:20	10:10	10:20	11:20	n/d	15:30	16:30	20:20
d_j	5:30	8:30	9:30	10:30	15:30	15:30	14:50	n/d	19:30	19:30	23:30
ID_i	1	2	3	1	2	3	1	n/a	1	2	1

Let us notice that the taxi EV₈ could not be served (i.e., its request was not accepted), all the three chargers already being in use at the EV₈ requested time; for that reason, the charger ID of the taxi EV₈ is marked as not available (n/a), and the variables corresponding to its arrival are marked as not defined (n/d).

In the following subsection, the behaviour of charger number 1 is analysed to benchmark the tested solution strategies, due to its high activity in this simulation (five electric vehicles served: EV₁, EV₄, EV₇, EV₉, and EV₁₁).

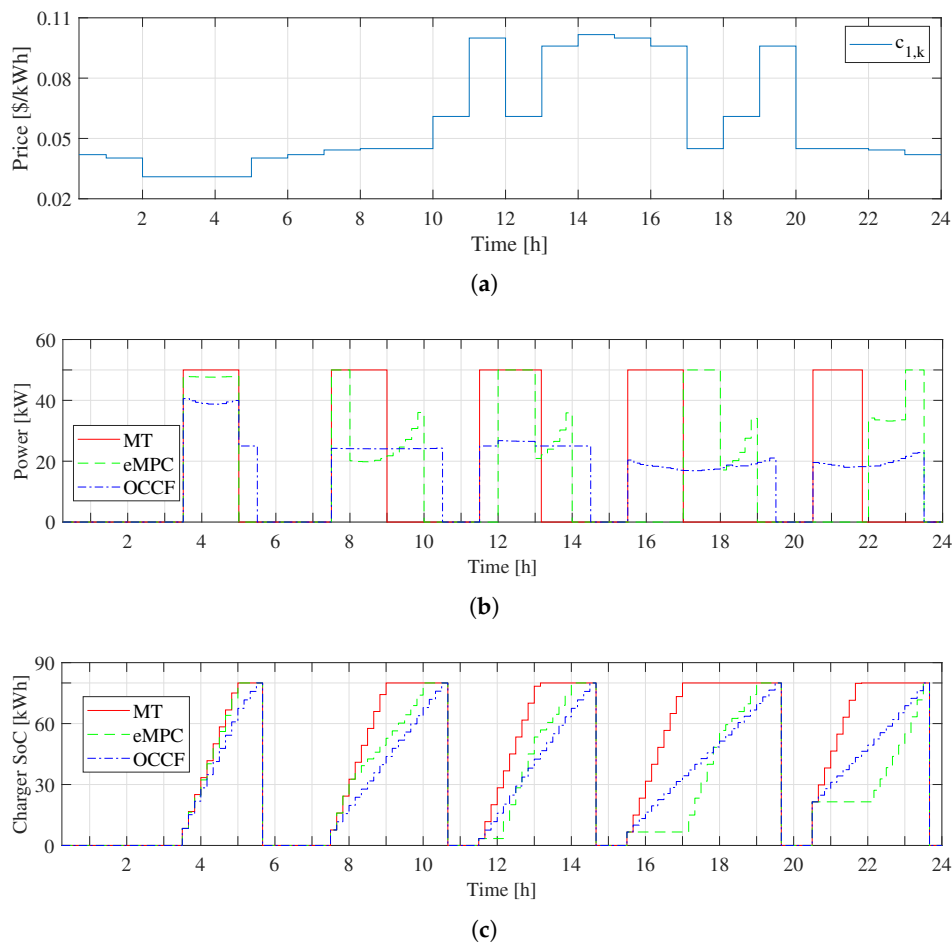


Figure 5. The behaviour of the three charging strategies in charger 1, considering only request parameters. (a) Energy price sequence $c_{1,k}$. (b) Power profiles $P_{1,k}$ with the different strategies. (c) Charger SoC $x_{1,k}$ with the different strategies.

4.1.1. Deterministic Performance

In order to perform a deterministic analysis of the proposed charging strategies, the first simulation campaign takes into account a full information approach. It is assumed that: (i) an Oracle informs the aggregator about the actual arrival SoC of each EV, i.e., it knows the information since the moment when a request is performed, that is, at least H hours in advance; and (ii) the EV arrival time is the one reported in the request.

In Figure 5, the most relevant aspects of the three charging strategies are shown and compared. Figure 5a depicts the simulated time-variable energy price sequence $c_{1,k}$ adopted in this simulation, as reported in Table 2. Figure 5b shows the power profile delivered by charger 1, namely $P_{1,k}$, to the 5 EVs it serves. As expected, the $P_{1,k}$ profiles are always positive or equal to zero. By definition, the MT strategy (red line) charges the vehicles with a constant power $P_{\max} = 50$ kW, until the battery SoC reaches a full condition, i.e., $x_{1,d_j} = 80$ kWh (100%). Conversely, the eMPC solution (dashed-green line) envisages different power levels taking into account the energy prices, while ensuring the 100% SoC target at the departure time. Finally, in the OCCF strategy (dash-dot blue line), the charging power is continuously adjusted while the algorithm tries to achieve the same upward and downward flexibility, by keeping $P_{1,k}$ close to a medium level, roughly 25 kW. Nevertheless, for EV₁, in Figure 5b, between the arrival time $a_1 = 3:30$ a.m. and the departure time $d_1 = 5:30$ a.m., a medium power level cannot be maintained, due to the shorter charging time (2 h) given by the EV owner request. In the last 30 min, the energy price increases, and the OCCF strategy takes into account this fact to schedule lower power in that period. Figure 5c shows the resulting SoC evolution, $x_{1,k}$, of the EVs served by the charger.

As expected, the MT strategy reaches a full charge condition faster. On the other side, by comparing Figure 5a,c, it is worthwhile to notice how the eMPC strategy strives to limit as much as possible its charging level at high price hours. Conversely, the OCCF solution, which depends on both flexibility and economic aspects, achieves a trade-off between energy cost reduction and flexibility generation.

Figure 6 depicts the charger 1 flexibility level, referring to the three strategies. The MT strategy cannot offer any upward flexibility capacity (U_{MT}), but it can offer a downward one ($-L_{MT}$). Conversely, the eMPC strategy has the possibility to offer an amount of upward (U_{eMPC}) and downward ($-L_{eMPC}$) flexibility, but it cannot provide both flexibilities at the same time for the majority of the time slots. However, the OCCF strategy according to the problem formulation (see Equation (19a) and Equation (19b)), which includes the flexibility in the cost function, offers both upward (U_{OCCF}) and downward ($-L_{OCCF}$) flexibilities at almost all the time steps when there is a connected EV.

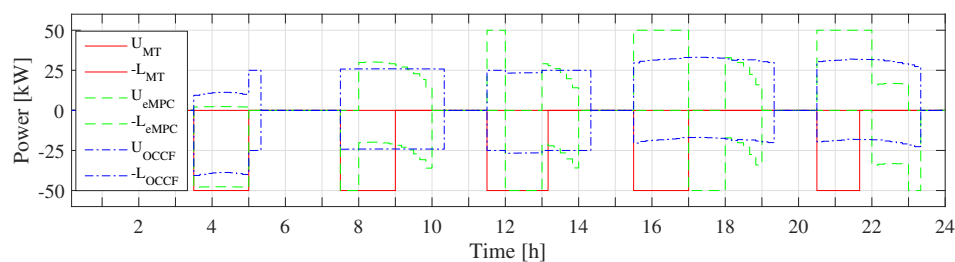


Figure 6. Flexibility capacity provided by charger 1.

From the results shown in Figure 6, it is clear that charger 1 can provide ancillary services to the grid, e.g., a spinning reserve service, for a relevant amount of time. The best option to offer this service is with the OCCF charging strategy. For example, by comparing the trends in Figs 5b and 6, let us notice that, between hours 13:10 and 14:20, the charger can offer its maximum flexibility capacity ($F_{1,k} = 25$ kW). Indeed, in that interval, the delivered charging power is roughly in the middle of the maximum one $P_{1,max} = 50$ kW. In different time intervals, no flexibility might exist (see Definition 1), for instance between hours 5:20 and 5:30 or 23:20 and 23:30.

To conclude, the overall results of this simulation campaign are summarised in Table 4—specifically, the total aggregator cost, the savings of the two MPC strategies with respect to the MT solution and both upper and downward flexibilities capacities. It can be seen how the OCCF solution, maximising the flexibility levels, is an attractive solution for the aggregator.

Table 4. Three strategies' overall simulation results (three chargers, 11 EV requests)

Strategy	Charging Cost [\$]	Cost Savings [%]	$U_{T,k}^F$ Capacity [kWh]	$L_{T,k}^F$ Capacity [kWh]
Minimum Time (MT)	272.55	—	0.00	4300.00
economic Model Predictive Control (eMPC)	216.98	20.39	3226.06	4073.94
Optimal Control with Minimum Cost and Maximum Flexibility (OCCF)	257.34	5.55	6097.77	3902.23

4.1.2. Results with Uncertainty in Arrival SoC and Arrival Time

In the second set of simulations, the same conditions of the previous subsection are maintained, considering the set up presented in Table 2. There is no oracle providing the exact EV information about arrival time a_j , departure time d_j , and initial SoC SoC_{j,a_j} . These parameters are generated randomly as described at the beginning of the section. Then, the eMPC and OCCF strategies can, in the prediction step, over or underestimate the time required to fully charge an EV. However, the feedback structure of the MPC solution is able to overcome the uncertainty as shown in the following.

Figure 7 shows the performance of the three charging strategies. Figure 7a shows the power trajectories $P_{1,k}$. Figure 7b shows the SoC $x_{1,k}$ of charger 1, where the purple asterisks (*) indicate the

reported arrival time \tilde{a}_j and EV SoC ($\widehat{\text{SoC}}_{j,r_j}$) at the request time, i.e., the expected arrival time with the maximum expected SoC at the arrival.

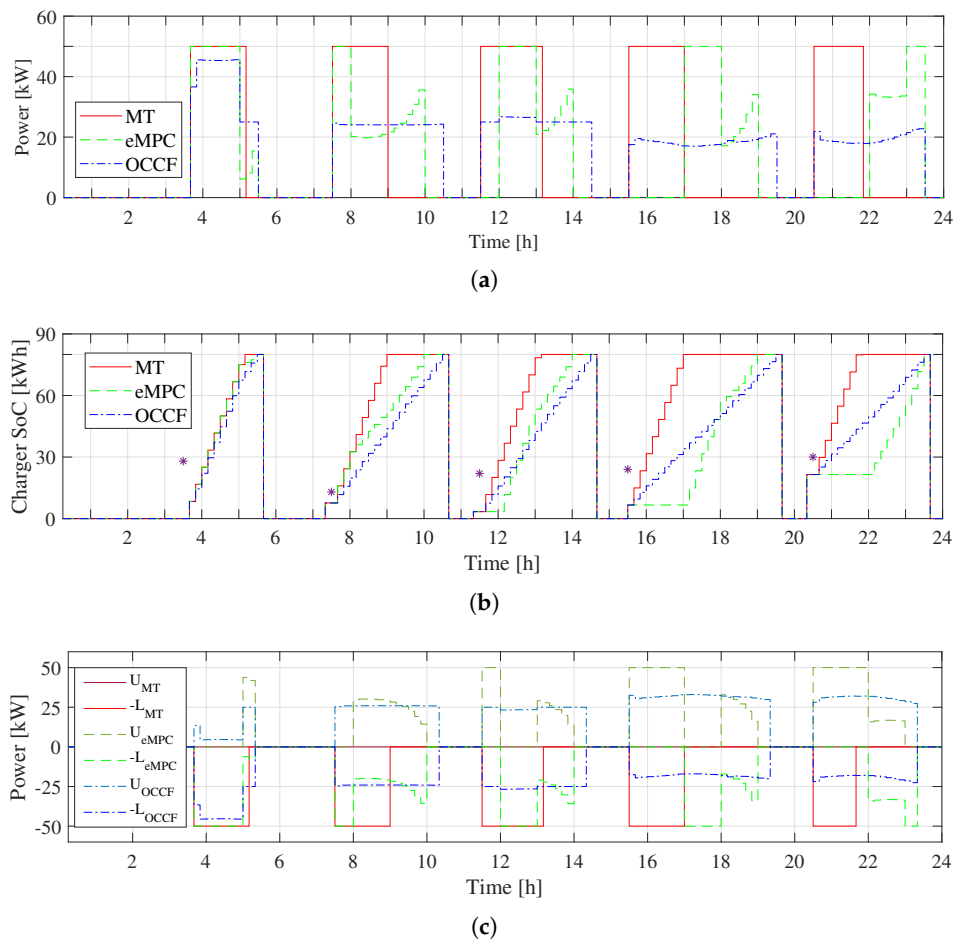


Figure 7. The behaviour of the three charging strategies in charger 1, with arrival SoC and time uncertainties. (a) Power profiles $P_{1,k}$ with the different strategies. (b) Charger SoC $x_{1,k}$ with the different strategies. (c) Flexibility capacity provided by charger 1.

Comparing the power consumptions in Figure 5b with the ones presented in Figure 7a, for strategies eMPC and OCCF, it can be seen that they have similar behaviours, especially when the prediction error is small, as for EVs 4, 7 and 11. However, for EVs 1 and 9, the prediction is far from the actual arrival SoC and the arrival time is also different. Note that the aggregator assumes that EV₁ ($a_1=3:40$, $d_1=5:30$) and EV₉ ($a_9=15:30$, $d_9=19:30$) were arriving with a high SoC. Then, the power curves show a peak during the first sample times, while the MPC strategies correct the mismatch; then, they follow an optimal charging profile, similar to the exact information case. Interestingly, the flexibility offered by charger 1, shown in Figure 7c, is just marginally affected by the prediction error. There is always a symmetric capacity, with a small deviation during the first sample times.

The results of the complete simulation (EVCS with all its chargers) are summarised in Table 5. The aggregator operation cost with different strategies is shown. In addition, the savings of the eMPC and OCCF strategies are calculated in comparison with the MT strategy. As expected, the OCCF strategy maximises the flexibility capacities. Furthermore, there is no relevant difference for the eMPC and OCCF strategies between knowing or not in advance the EV arrival SoC. Indeed, for this case, the charging cost for the eMPC strategy increases by just 0.17%, while, for the OCCF, it increases by 0.06%. Therefore, this suggests that the MPC strategies are robust in front of the EV arrival time and initial SoC information.

Table 5. Strategies' overall simulation results, with uncertainty in the arrival time and initial SoC (three chargers, 11 EV requests).

Strategy	Charging Cost (\$)	Cost Savings (%)	U_T^F Capacity (kWh)	L_T^F Capacity (kWh)
MT	272.63	-	0.00	4300.00
eMPC	217.34	20.27	3241.46	4058.54
OCCF	257.50	5.54	5997.95	3902.05

4.2. Savings, Benefits, and Flexibility in the EVCS

Now that the main characteristics of the proposed strategies have been highlighted in a small example, an extensive simulation campaign is presented, reproducing an EVCS with 25 chargers and 110 EV re-charge requests to be fulfilled in one day. These simulations are developed considering uncertainty in the arrival SoC and arrival time. The main results are shown in Figure 8. In Figure 8a, the number of EVs arriving at the station (red line) and the number of EVs connected (dashed-blue line) at each time slot are shown. In Figure 8b, the time history of the delivered charging power is shown for the three solution strategies. Consistently with the preliminary case, the OCCF solution generates the smoothest behaviour. Then, Figure 8c focuses on the overall station operational cost at each time slot. Specifically, it provides further evidence that, although the eMPC strategy might be the more expensive one at certain time intervals, by considering the overall daily operations, it is the cheapest solution. This is in line with the preliminary results listed in Table 5.

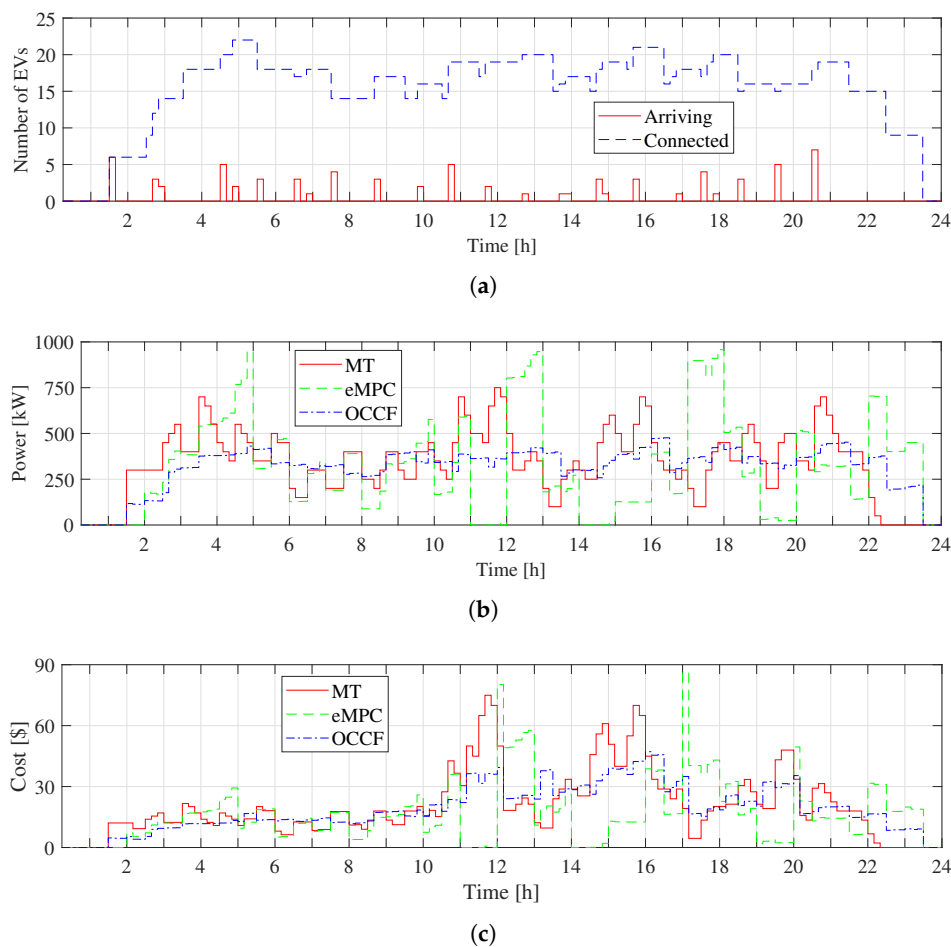
**Figure 8.** The behaviour of the three charging strategies in the EVCS. (a) EV arrival and EVs connected in the operational time. (b) Power delivered. (c) EVCS cost.

Figure 9 shows the flexibility capacity that the EVCS can offer to the system operator at each time slot k , with the three strategies, along the operation time of the station. As already mentioned, the upward and the downward flexibilities in the OCCF strategy are maximised, according to the optimal problem formulation. Interestingly, by comparing this simulated result with the outcome in Figure 7c, the OCCF strategy offers a certain level of flexibility at every time interval, allowing for providing spinning reserve service to the grid all day long. This evidence suggests that the more EVs are connected, the higher is the algorithm capability to achieve charging flexibility.

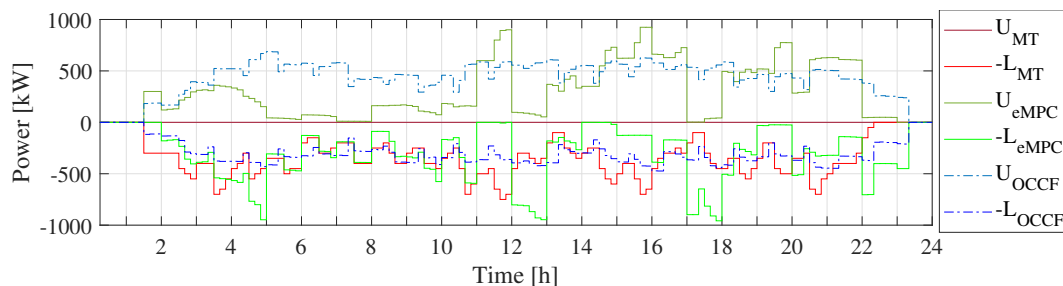


Figure 9. EVCS flexibility capacity.

To sum up, Table 6 lists the overall results of this second simulation scenario. Once again, it is shown that the higher flexibility capacity levels are achieved by the OCCF solution. Concerning the savings of the MPC solutions with respect to the MT strategy, the values are of the same order of magnitude of the preliminary case in Table 4. This might imply that those savings are independent of the amount of plugged-in EVs, yet dictated by the chosen solution strategy and energy price evolution.

Table 6. Three strategies’ overall simulation results, considering uncertainties (25 chargers, 110 EV requests).

Strategy	Charging Cost (\$)	Cost Savings (%)	$U_{T,k}^F$ Capacity (kWh)	$L_{T,k}^F$ Capacity (kWh)
MT	2913.13	-	0.0	47,600.00
eMPC	2322.36	20.28	40,979.68	42,620.32
OCCF	2706.40	7.10	61,059.26	42,240.74

4.3. Monte Carlo Analysis

The performance of the proposed EVCS operation strategies is evaluated through a Monte Carlo simulation, where the EVs SoC, arrival and departure times are randomised, and the resulting overall savings with respect to the outcomes of the MT strategy are analysed. To this aim, the optimal decision problem for an EVCS with 25 chargers and 110 EV requests is solved for 500 realisations of random EV arrival and departure times, a_j and d_j . In more detail, the EV arrival flow is assumed to be a random variable with uniform distribution during the day, considering that electric taxis operate 24 h and can be charged at any time. Then, in the simulation, \tilde{a}_j is generated as a random variable, with uniform distribution between hour 1:30 a.m. and hour 20:30. Note that, for another type of user, it would be possible to identify the distribution that better represents it [74], for example, analysing historical data [75]. Moreover, d_j is also randomly generated, constrained to guarantee a charging time between $2 \div 6$ h; 2 h is the minimum interval guaranteeing a feasible charging procedure, and 6 h as a reasonable time for resting between work shifts. Two price sequences, $c_{1,k}$ and $c_{2,k}$ as per Table 2, are considered, allowing for evaluating the sensitivity of the strategies to the energy cost.

In the MT and eMPC strategies, no remuneration factor is considered. In particular, the results of the eMPC strategy are to avoid or reduce the consumption at high energy prices, thus increasing the upward capacity available and reducing the downward capacity available. This available capacity is calculated from a purely technical point of view. Conversely, the OCCF algorithm, as per the

Formulation Equation (19), finds a trade-off between energy cost and flexibility capacity, thus distributing the energy consumption throughout all the time-slots. In turn, this leads to a schedule with the EV charging station operating during high-cost hours, thus making the overall charging process more expensive but guaranteeing an almost symmetrical flexibility at all times.

In the OCCF strategy, the remuneration is given to provide flexibility. The remuneration factor is assumed to be higher when the energy price is high because, without an appropriate incentive, nobody would provide flexibility in the higher energy price periods. Thereby, it is reasonable that the trend of the remuneration factor follows the energy price sequence.

A comparison is introduced here in the form of parametric analysis, in which the remuneration factor is chosen at different percentages of the energy prices. In this way, the overall cost savings of providing flexibility with respect to the MT strategy are quantified. When the price sequence $c_{1,k}$ (see Figure 5a) is considered in the Monte Carlo simulation, the probability density function (PDF) of the overall savings is shown in Figure 10. The other cases for the OCCF strategy are formulated with remuneration factors of 10%, 20%, and 30% of the energy price (the further case with 100% is not shown but is included in Table 7). By definition, with null remuneration factor, the solution is the same as in the eMPC. By introducing remuneration, the energy costs of the different solutions increase, but the benefits due to remuneration are higher, and the solutions become more profitable. Indeed, when the remuneration is equal to the energy price, the overall savings are very high (even though these savings refer to the MT strategy, such values higher than 100% are conceptually feasible).

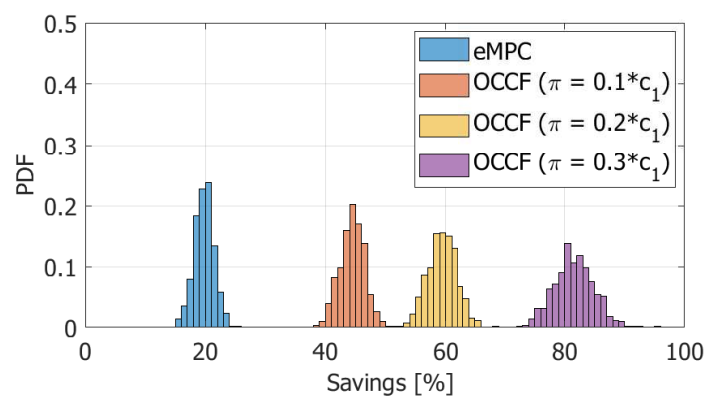


Figure 10. Overall savings for different strategies and remuneration factors based on c_1 .

When the energy price sequence $c_{2,k}$ is used (Figure 11), the most relevant outcomes of the Monte Carlo trials are shown in Figure 12.

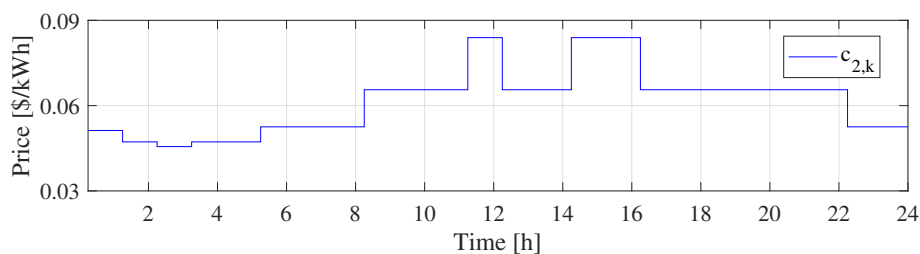


Figure 11. Energy price sequence $c_{2,k}$.

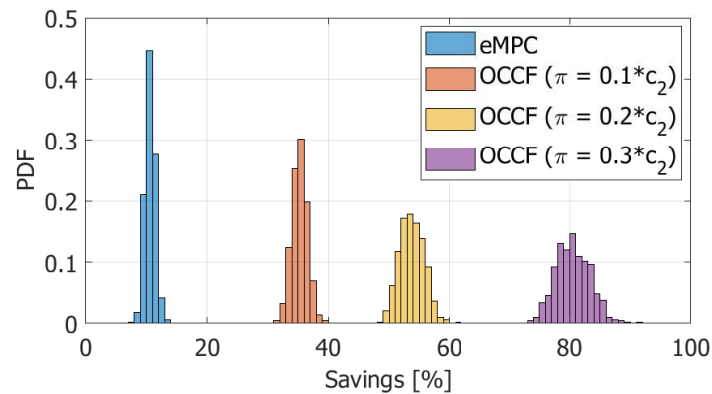


Figure 12. Overall savings for different strategies and remuneration factors based on c_2 .

The results summarised in Table 7 show that the average savings for the set-up with price $c_{1,k}$ are higher than for the price $c_{2,k}$. This can be explained by the difference in the ratio between the standard deviation and the mean value of the energy prices, 0.44 for $c_{1,k}$ and 0.19 for $c_{2,k}$ (see Table 2). Hence, the higher the variability of the energy cost profile, the higher the capability of the MPC strategies to achieve more convenient schedules on a daily basis, charging the vehicles principally at the cheapest time slots. When the remuneration factor increases, the mean overall savings increase, and the standard deviation of the overall savings also increases. Furthermore, the overall savings found starting from the two different energy price sequences tend to be similar when the remuneration factor increases. This is due to the fact that, with high remuneration factors, the power profiles tend to be more constant (see Figures 7a and 8b). This happens already when the remuneration factor is 30% of the energy price for the two energy price sequences, and, for this reason, the results shown in Figures 10 and 12 are shown up to 30%.

Table 7. Mean value and standard deviation of the overall savings with respect to the MT strategy.

Strategy and Remuneration Factor	Overall Savings		Strategy and Remuneration Factor	Overall Savings	
	Mean (%)	Std (%)		Mean (%)	Std (%)
eMPC, $\pi = 0$	19.8	1.6	eMPC, $\pi = 0$	10.6	0.8
OCCF, $\pi = 0.1 \cdot c_1$	44.5	2.1	OCCF, $\pi = 0.1 \cdot c_2$	35.3	1.3
OCCF, $\pi = 0.2 \cdot c_1$	59.5	2.4	OCCF, $\pi = 0.2 \cdot c_2$	53.9	2.2
OCCF, $\pi = 0.3 \cdot c_1$	81.6	3.4	OCCF, $\pi = 0.3 \cdot c_2$	80.6	3.0
OCCF, $\pi = c_1$	257.9	10.2	OCCF, $\pi = c_2$	257.9	10.1

5. Conclusions

This work has proposed two novel strategies for the scheduling of the charging power of a Electric Vehicle Charging Station (EVCS) that can be used by an aggregator. The first strategy looks for minimising the EVCS operation costs via an economic Model Predictive Control (eMPC). The second strategy develops an Optimal Control with minimum Cost and maximum Flexibility (OCCF) formulation, where the EV charger flexibility capacity is defined as the power deviations attainable by the charger with respect to a given nominal charging profile. Following a smart grid standard approach for charging EVs, these strategies can adjust the power at each time slot, which could be carried out through available technologies and solutions such as the open charge point protocol. In both eMPC and OCCF strategies, the effect of uncertainty on the arrival time and on the state of charge of the EV battery at the arrival are taken into account. The two charging strategies were benchmarked against the simple Minimum Time (MT) charging strategy. Interestingly, the OCCF charging strategy was found not only to reduce the EVCS operating costs with respect to the MT benchmark case, but also to maximise the load profile flexibility, giving the possibility of offering ancillary services to the grid, like spinning reserve, through upward/downward power deviations at each time slot. In addition, a dynamic model of an EVCS charger as a flexible load was developed.

The model has a switching behaviour, according to whether there is an EV plugged in to the charger or not.

A wide range of numerical simulations based on the electric taxi service used in Bogotá (Colombia) were presented, considering two sequences of energy spot prices, taken from the Colombian market. We found that, in all cases, the two proposed strategies reduce the operation costs with respect to a minimum charging time solution, although the time spent at the station premises is increased. However, the OCCF strategy is slightly more expensive. It was shown that the cost reduction is not affected when the arrival time and SoC of the EVs are not precisely known in advance.

While the eMPC solutions offer some flexibility in the power demand, the upward and downward flexibility capacity offered by the OCCF strategy is more balanced, has smooth variations during the day and limits the power peaks that may occur with the other strategies. As such, the OCCF strategy becomes of particular interest for the EVCS to benefit from offering ancillary services through demand response programs, generating additional revenues.

As future work, the strategies used by the aggregator will be improved by considering renewable sources providing energy to the charging station as well as the use of real data of EV usage. In addition, longer time periods of analysis will be considered and the EV battery degradation cost will be included in the optimization cost function. However, these future features do not modify the proposed formulation of the flexibility.

Author Contributions: All authors contributed equally to conceptualization, methodology development, software implementation, validation, formal analysis, investigation, writing-original draft preparation, writing-review and editing, visualization, and supervision.

Funding: This research received no external funding.

Acknowledgments: C.D.-L. received a doctoral scholarship from the program “Rodolfo Llinás para la promoción de la formación avanzada y el espíritu científico en Bogotá” from *Secretaría de Desarrollo Económico de Bogotá* and *Fundación CEIBA*. F.R. thanks the Politecnico di Torino for the invitation as a Visiting professor, where part of this work was developed.

Conflicts of Interest: The authors declare no conflict of interest.

References

1. U.S. Energy Information Administration. International Energy Outlook 2017. Technical Report. 2017. Available online: [www.eia.gov/forecasts/ieo/pdf/0484\(2016\).pdf](http://www.eia.gov/forecasts/ieo/pdf/0484(2016).pdf) (accessed on 11 September 2019).
2. Nghitevelekwa, K.; Bansal, R.C. A review of generation dispatch with large-scale photovoltaic systems. *Renew. Sustain. Energy Rev.* **2018**, *81*, 615–624. [[CrossRef](#)]
3. Bakirtzis, E.A.; Simoglou, C.K.; Biskas, P.N.; Bakirtzis, A.G. Storage management by rolling stochastic unit commitment for high renewable energy penetration. *Electr. Power Syst. Res.* **2018**, *158*, 240–249. [[CrossRef](#)]
4. Pandurangan, V.; Zareipour, H.; Malik, O. Frequency Regulation Services : A Comparative Study of Select North American and European Reserve Markets. In Proceedings of the 2012 North American Power Symposium (NAPS), Champaign, IL, USA, 9–11 September 2012; pp. 1–8.
5. Deng, R.; Yang, Z.; Chow, M.Y.; Chen, J. A Survey on Demand Response in Smart Grids: Mathematical Models and Approaches. *IEEE Trans. Ind. Inform.* **2015**, *11*, 570–582. [[CrossRef](#)]
6. Ma, J.; Silva, V.; Belhomme, R.; Kirschen, D.S.; Ochoa, L.F. Evaluating and Planning Flexibility in Sustainable Power Systems. *IEEE Trans. Sustain. Energy* **2013**, *4*, 200–209. [[CrossRef](#)]
7. Holttinen, H.; Tuohy, A.; Milligan, M.; Silva, V.; Müller, S.; Söder, L. The Flexibility Workout: Managing Variable Resources and Assessing the Need for Power System Modification. *IEEE Power Energy Mag.* **2013**, *11*, 53–62. [[CrossRef](#)]
8. Ulbig, A.; Andersson, G. Analyzing operational flexibility of electric power systems. *Int. J. Electr. Power Energy Syst.* **2015**, *72*, 155–164. [[CrossRef](#)]
9. Li, J.; Liu, F.; Li, Z.; Shao, C.; Liu, X. Grid-side flexibility of power systems in integrating large-scale renewable generations: A critical review on concepts, formulations and solution approaches. *Renew. Sustain. Energy Rev.* **2018**, *93*, 272–284. [[CrossRef](#)]

10. Hao, H.; Sanandaji, B.M.; Poolla, K.; Vincent, T.L. Aggregate Flexibility of Thermostatically Controlled Loads. *IEEE Trans. Power Syst.* **2015**, *30*, 189–198. [[CrossRef](#)]
11. Zhao, L.; Zhang, W. A Geometric Approach to Aggregate Flexibility Modeling of Thermostatically Controlled Loads. *IEEE Trans. Power Syst.* **2017**, *32*, 4721–4731. [[CrossRef](#)]
12. Sajjad, I.A.; Chicco, G.; Napoli, R. Definitions of Demand Flexibility for Aggregate Residential Loads. *IEEE Trans. Smart Grid* **2016**, *7*, 2633–2643. [[CrossRef](#)]
13. Diaz, C.; Ruiz, F.; Patino, D. Modeling and control of water booster pressure systems as flexible loads for demand response. *Appl. Energy* **2017**, *204*, 106–116. [[CrossRef](#)]
14. Papadaskalopoulos, D.; Strbac, G.; Mancarella, P.; Aunedi, M.; Stanojevic, V. Decentralized Participation of Flexible Demand in Electricity Markets—Part II : Application With Electric Vehicles and Heat Pump Systems. *IEEE Trans. Power Syst.* **2013**, *28*, 3667–3674. [[CrossRef](#)]
15. Good, N.; Mancarella, P. Flexibility in multi-energy communities with electrical and thermal storage: A stochastic, robust approach for multi-service demand response. *IEEE Trans. Smart Grid* **2019**, *10*, 503–513. [[CrossRef](#)]
16. Wang, Y.; Cheng, J.; Zhang, N.; Kang, C. Automatic and linearized modeling of energy hub and its flexibility analysis. *Appl. Energy* **2018**, *211*, 705–714. [[CrossRef](#)]
17. Haas, J.; Cebulla, F.; Cao, K.; Nowak, W.; Palma-behnke, R.; Rahmann, C.; Mancarella, P. Challenges and trends of energy storage expansion planning for flexibility provision in low-carbon power systems—A review. *Renew. Sustain. Energy Rev.* **2017**, *80*, 603–619. [[CrossRef](#)]
18. Pavić, I.; Capuder, T.; Kuzle, I. Value of flexible electric vehicles in providing spinning reserve services. *Appl. Energy* **2015**, *157*, 60–74. [[CrossRef](#)]
19. Borba, B.S.M.; Szklo, A.; Schaeffer, R. Plug-in hybrid electric vehicles as a way to maximize the integration of variable renewable energy in power systems: The case of wind generation in northeastern Brazil. *Energy* **2012**, *37*, 469–481. [[CrossRef](#)]
20. Khemakhem, S.; Rekik, M.; Krichen, L. A flexible control strategy of plug-in electric vehicles operating in seven modes for smoothing load power curves in smart grid. *Energy* **2017**, *118*, 197–208. [[CrossRef](#)]
21. Wenzel, G.; Negrete-pincetic, M.; Olivares, D.E.; Macdonald, J.; Callaway, D.S. Real-Time Charging Strategies for an Electric Vehicle Aggregator to Provide Ancillary Services. *IEEE Trans. Smart Grid* **2018**, *9*, 5141–5151. [[CrossRef](#)]
22. Giordano, F.; Ciocia, A.; Di Leo, P.; Spertino, F.; Tenconi, A.; Vaschetto, S. Self-Consumption Improvement for a Nanogrid with Photovoltaic and Vehicle-to-Home Technologies. In Proceedings of the 2018 IEEE International Conference on Environment and Electrical Engineering and 2018 IEEE Industrial and Commercial Power Systems Europe (EEEIC/I&CPS Europe), Palermo, Italy, 12–15 June 2018; pp. 1–6.
23. Noel, L.; Rubens, G.Z.D.; Sovacool, B.K. Optimizing innovation, carbon and health in transport: Assessing socially optimal electric mobility and vehicle-to-grid pathways in Denmark. *Energy* **2018**, *153*, 628–637. [[CrossRef](#)]
24. Cao, Y.; Wang, T.; Kaiwartya, O.; Min, G.; Ahmad, N.; Abdullah, A.H. An EV Charging Management System Concerning Drivers' Trip Duration and Mobility Uncertainty. *IEEE Trans. Syst. Man Cybern. Syst.* **2018**, *48*, 596–607. [[CrossRef](#)]
25. García-Villalobos, J.; Zamora, I.; San Martín, J.I.; Asensio, F.J.; Aperribay, V. Plug-in electric vehicles in electric distribution networks: A review of smart charging approaches. *Renew. Sustain. Energy Rev.* **2014**, *38*, 717–731. [[CrossRef](#)]
26. Quirós-Tortós, J.; Ochoa, L.; Butler, T. How Electric Vehicles and the Grid Work Together: Lessons Learned from One of the Largest Electric Vehicle Trials in the World. *IEEE Power Energy Mag.* **2018**, *16*, 64–76. [[CrossRef](#)]
27. Haidar, A.M.A.; Muttaqi, K.M.; Haque, M.H. Multistage time-variant electric vehicle load modelling for capturing accurate electric vehicle behaviour and electric vehicle impact on electricity distribution grids. *IET Gener. Transm. Distrib.* **2015**, *9*, 2705–2716. [[CrossRef](#)]
28. Sundström, O.; Binding, C. Flexible charging optimization for electric vehicles considering distribution grid constraints. *IEEE Trans. Smart Grid* **2012**, *3*, 26–37. [[CrossRef](#)]

29. Hu, J.; Morais, H.; Sousa, T.; Lind, M. Electric vehicle fleet management in smart grids: A review of services, optimization and control aspects. *Renew. Sustain. Energy Rev.* **2016**, *56*, 1207–1226. [[CrossRef](#)]
30. Schuller, A.; Flath, C.M.; Gottwalt, S. Quantifying load flexibility of electric vehicles for renewable energy integration. *Appl. Energy* **2015**, *151*, 335–344. [[CrossRef](#)]
31. Sadeghianpourhamami, N.; Refa, N.; Strobbe, M.; Develder, C. Quantitative analysis of electric vehicle flexibility: A data-driven approach. *Int. J. Electr. Power Energy Syst.* **2018**, *95*, 451–462. [[CrossRef](#)]
32. Mills, G.; Macgill, I. Assessing Electric Vehicle storage, flexibility, and Distributed Energy Resource potential. *J. Energy Storage* **2018**, *17*, 357–366. [[CrossRef](#)]
33. Munshi, A.A.; Mohamed, Y. Extracting and Defining Flexibility of Residential Electrical Vehicle Charging Loads. *IEEE Trans. Ind. Inform.* **2018**, *14*, 448–461, [[CrossRef](#)]
34. Grahn, P.; Alvehag, K.; Söder, L. PHEV Utilization Model Considering Type-of-Trip and Recharging Flexibility. *IEEE Trans. Smart Grid* **2014**, *5*, 139–148, [[CrossRef](#)]
35. Clairand, J.M.; Rodríguez-García, J.; Álvarez-Bel, C. Smart Charging for Electric Vehicle Aggregators Considering Users' Preferences. *IEEE Access* **2018**, *6*, 54624–54635. [[CrossRef](#)]
36. Qi, W.; Xu, Z.; Shen, Z.J.M.; Hu, Z.; Song, Y. Hierarchical coordinated control of plug-in electric vehicles charging in multifamily dwellings. *IEEE Trans. Smart Grid* **2014**, *5*, 1465–1474. [[CrossRef](#)]
37. Yang, L.; Zhang, J.; Poor, H.V. Risk-aware day-ahead scheduling and real-time dispatch for electric vehicle charging. *IEEE Trans. Smart Grid* **2014**, *5*, 693–702. [[CrossRef](#)]
38. Janjic, A.; Velimirovic, L.; Stankovic, M.; Petrusic, A. Commercial electric vehicle fleet scheduling for secondary frequency control. *Electr. Power Syst. Res.* **2017**, *147*, 31–41. [[CrossRef](#)]
39. Wang, R.; Xiao, G.; Wang, P. Hybrid Centralized-Decentralized (HCD) Charging Control of Electric Vehicles. *IEEE Trans. Veh. Technol.* **2017**, *66*, 6728–6741. [[CrossRef](#)]
40. Pertl, M.; Carducci, F.; Tabone, M.; Marinelli, M.; Kiliccote, S.; Kara, E.C. An Equivalent Time-Variant Storage Model to Harness EV Flexibility : Forecast and Aggregation. *IEEE Trans. Ind. Inform.* **2019**, *15*, 1899–1910. [[CrossRef](#)]
41. Esmaili, M.; Goldoust, A. Multi-objective optimal charging of plug-in electric vehicles in unbalanced distribution networks. *Int. J. Electr. Power Energy Syst.* **2015**, *73*, 644–652. [[CrossRef](#)]
42. Škugor, B.; Deur, J. Dynamic programming-based optimisation of charging an electric vehicle fleet system represented by an aggregate battery model. *Energy* **2015**, *92*, 456–465. [[CrossRef](#)]
43. Sun, B.; Tan, X.; Tsang, D.H.K. Eliciting Multi-dimensional Flexibilities from Electric Vehicles: A Mechanism Design Approach. *IEEE Trans. Power Syst.* **2018**. [[CrossRef](#)]
44. Zhou, B.; Yao, F.; Littler, T.; Zhang, H. An electric vehicle dispatch module for demand-side energy participation. *Appl. Energy* **2016**, *177*, 464–474. [[CrossRef](#)]
45. del Razo, V.; Goebel, C.; Jacobsen, H.A. Vehicle-Originating-Signals for Real-Time Charging Control of Electric Vehicle Fleets. *IEEE Trans. Transp. Electrification* **2015**, *1*, 150–167. [[CrossRef](#)]
46. Su, W.; Wang, J.; Zhang, K.; Huang, A.Q. Model predictive control-based power dispatch for distribution system considering plug-in electric vehicle uncertainty. *Electr. Power Syst. Res.* **2014**, *106*, 29–35. [[CrossRef](#)]
47. Ruelens, F.; Vandael, S.; Leterme, W.; Claessens, B.J.; Hommelberg, M.; Holvoet, T.; Belmans, R. Demand side management of electric vehicles with uncertainty on arrival and departure times. In Proceedings of the IEEE PES Innovative Smart Grid Technologies Conference Europe, Berlin, Germany, 14–17 October 2012; pp. 1–8. [[CrossRef](#)]
48. Ji, Z.; Huang, X.; Xu, C.; Sun, H. Accelerated model predictive control for electric vehicle integrated microgrid energy management: A hybrid robust and stochastic approach. *Energies* **2016**, *9*, 973. [[CrossRef](#)]
49. Halvgaard, R.; Poulsen, N.K.; Madsen, H.; Jørgensen, J.B.; Marra, F.; Bondy, D.E.M. Electric vehicle charge planning using economic model predictive control. In Proceedings of the 2012 IEEE International Electric Vehicle Conference (IEVC 2012), Greenville, SC, USA, 4–8 March 2012; pp. 1–6. [[CrossRef](#)]
50. Diaz, C.; Ruiz, F.; Patino, D. Smart Charge of an Electric Vehicles Station: A Model Predictive Control Approach. In Proceedings of the 2018 IEEE Conference on Control Technology and Applications (CCTA), Copenhagen, Denmark, 21–24 August 2018; pp. 54–59. [[CrossRef](#)]
51. Diaz, C.; Mazza, A.; Ruiz, F.; Patino, D.; Chicco, G. Understanding Model Predictive Control for Electric Vehicle Charging Dispatch. In Proceedings of the 2018 53rd International Universities Power Engineering Conference (UPEC), Glasgow, UK, 4–7 September 2018; pp. 1–6.

52. Braun, M.W.; Rivera, D.E.; Carlyle, W.M.; Kempf, K.G. A model predictive control framework for robust management of multi-product, multi-echelon demand networks. *IFAC Proc. Vol. (IFAC-PapersOnline)* **2003**, *27*, 229–245. [[CrossRef](#)]
53. Oldewurtel, F.; Parisio, A.; Jones, C.N.; Gyalistras, D.; Gwerder, M.; Stauch, V.; Lehmann, B.; Morari, M. Use of model predictive control and weather forecasts for energy efficient building climate control. *Energy Build.* **2012**, *45*, 15–27. [[CrossRef](#)]
54. Colmenar-Santos, A.; Muñoz-Gómez, A.M.; Rosales-Asensio, E.; López-Rey, Á. Electric vehicle charging strategy to support renewable energy sources in Europe 2050 low-carbon scenario. *Energy* **2019**, *183*, 61–74. [[CrossRef](#)]
55. Naharudinsyah, I.; Limmer, S. Optimal Charging of Electric Vehicles with Trading on the Intraday Electricity Market. *Energies* **2018**, *11*, 1416. [[CrossRef](#)]
56. Mouli, G.R.C.; Kaptein, J.; Bauer, P.; Zeman, M. Implementation of dynamic charging and V2G using Chademo and CCS/Combo DC charging standard. In Proceedings of the 2016 IEEE Transportation Electrification Conference and Expo (ITEC 2016), Dearborn, MI, USA, 27–29 June 2016; pp. 1–6. [[CrossRef](#)]
57. Open Charge Alliance. Open Charge Point Protocol 1.6. Technical Report. 2015. Available online: <https://www.openchargealliance.org/> (accessed on 11 September 2019).
58. Amjad, M.; Ahmad, A.; Rehmani, M.H.; Umer, T. A review of EVs charging: From the perspective of energy optimization, optimization approaches, and charging techniques. *Transp. Res. Part Transp. Environ.* **2018**, *62*, 386–417. [[CrossRef](#)]
59. Hoke, A.; Brissette, A.; Smith, K.; Pratt, A. Accounting for Lithium-Ion Battery Degradation in Electric Vehicle Charging Optimization. *IEEE J. Emerg. Sel. Top. Power Electron.* **2014**, *2*, 691–700. [[CrossRef](#)]
60. Ottesen, S.Ø.; Tomasgard, A.; Fleten, S.E. Multi market bidding strategies for demand side flexibility aggregators in electricity markets. *Energy* **2018**, *149*, 120–134. [[CrossRef](#)]
61. Lund, P.D.; Lindgren, J.; Mikkola, J.; Salpakari, J. Review of energy system flexibility measures to enable high levels of variable renewable electricity. *Renew. Sustain. Energy Rev.* **2015**, *45*, 785–807. [[CrossRef](#)]
62. González, P.; Villar, J.; Díaz, C.A.; Campos, F.A. Joint energy and reserve markets: Current implementations and modeling trends. *Electr. Power Syst. Res.* **2014**, *109*, 101–111. [[CrossRef](#)]
63. Baccino, F.; Conte, F.; Massucco, S.; Silvestro, F.; Grillo, S. Frequency Regulation by Management of Building Cooling Systems through Model Predictive Control. In Proceedings of the 18th Power Systems Computation Conference (PSCC), Wroclaw, Poland, 18–22 August 2014; pp. 1–7. [[CrossRef](#)]
64. PJM Forward Market Operations. *PJM Manual 11: Energy and Ancillary Services Market Operations*; PJM: Audubon, PA, USA, 23 March 2017.
65. ISO New England Inc. *Operating Reserves White Paper*; ISO New England Inc.: Holyoke, MA, USA, 2006.
66. Kirby, B.J. *Frequency Regulation Basics and Trends*; U.S. Department of Energy: Washington, DC, USA, 2004; pp. 1–32.
67. Kirby, B.; Kueck, J.; Laughner, T.; Morris, K. *Spinning Reserve from Hotel Load Response: Initial Progress*; Oak Ridge National Laboratory: Oak Ridge, TN, USA, 2008; pp. 1–35.
68. Kara, E.C.; Tabone, M.D.; MacDonald, J.S.; Callaway, D.S.; Kiliccote, S. Quantifying flexibility of residential thermostatically controlled loads for demand response: A data-driven approach. In Proceedings of the 1st ACM Conference on Embedded Systems for Energy-Efficient Buildings, Memphis, TN, USA, 3–6 November 2014; pp. 140–147. [[CrossRef](#)]
69. Quinn, C.; Zimmerle, D.; Bradley, T.H. The effect of communication architecture on the availability, reliability, and economics of plug-in hybrid electric vehicle-to-grid ancillary services. *J. Power Sources* **2010**, *195*, 1500–1509. [[CrossRef](#)]
70. Kirby, B.; Hirst, E. *Customer-Specific Metrics for the Regulation and Load-Following Ancillary Services*; Technical Report; Oak Ridge National Laboratory: Oak Ridge, TN, USA, 2000. [[CrossRef](#)]
71. Yilmaz, M.; Krein, P.T. Review of charging power levels and infrastructure for plug-in electric and hybrid vehicles. *IEEE Trans. Power Electron.* **2013**, *28*, 2151–2169. [[CrossRef](#)]
72. Grant, M.; Boyd, S. CVX: Matlab Software for Disciplined Convex Programming. Version 2.1. 2014. Available online: www.cvxr.com/cvx (accessed on 11 September 2019).
73. CREG. Resolución Creg 209 de 2015, Bogotá Colombia. 2015. Available online: www.creg.gov.co (accessed on 11 September 2019).

74. Flammini, M.G.; Prettico, G.; Julea, A.; Fulli, G.; Mazza, A.; Chicco, G. Statistical characterisation of the real transaction data gathered from electric vehicle charging stations. *Electr. Power Syst. Res.* **2019**, *166*, 136–150. [[CrossRef](#)]
75. Bascetta, L.; Grusso, G.; Storti Gajani, G. Analysis of Electrical Vehicle behavior from real world data: A V2I Architecture. In Proceedings of the 2018 International Conference of Electrical and Electronic Technologies for Automotive AEIT, Milan, Italy, 9–11 July 2018; pp. 1–4.



© 2019 by the authors. Licensee MDPI, Basel, Switzerland. This article is an open access article distributed under the terms and conditions of the Creative Commons Attribution (CC BY) license (<http://creativecommons.org/licenses/by/4.0/>).